Journal Pre-proof

Identification of *N*-phenyl-3-methoxy-4-pyridinones as orally bioavailable H_3 receptor antagonists and β-amyloid aggregation inhibitors for the treatment of Alzheimer's disease

Minkui Zhang, Li Tang, Liu Jiang, Jun Wei, Yongzhou Hu, Rong Sheng

PII: S0223-5234(20)31068-0

DOI: https://doi.org/10.1016/j.ejmech.2020.113096

Reference: EJMECH 113096

To appear in: *European Journal of Medicinal Chemistry*

Received Date: 27 August 2020

Revised Date: 19 November 2020

Accepted Date: 8 December 2020

Please cite this article as: M. Zhang, L. Tang, L. Jiang, J. Wei, Y. Hu, R. Sheng, Identification of *N*-phenyl-3-methoxy-4-pyridinones as orally bioavailable H_3 receptor antagonists and β-amyloid aggregation inhibitors for the treatment of Alzheimer's disease, *European Journal of Medicinal Chemistry*, https://doi.org/10.1016/j.ejmech.2020.113096.

Graphical abstract

Identification of N-phenyl-3-methoxy-4-pyridinones as orally bioavailable H3 receptor antagonists and β-amyloid aggregation inhibitors for the treatment of Alzheimer's disease

Minkui Zhang[#], Li Tang[#], Liu Jiang, Jun Wei, Yongzhou Hu, Rong Sheng[*]

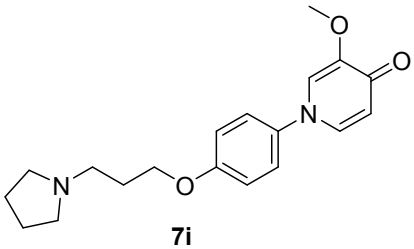

7i

hH_3R IC_{50} = 0.52 nM
$A\beta_{1-40}/A\beta_{1-42}$ aggregation inhibition
Oral bioavaliablity 47.9%
Good BBB permeability
Excellent subtypes selectivity
Low hERG channel inhibition risk

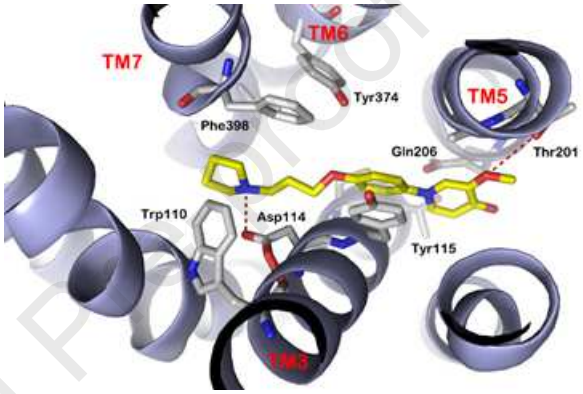

The binding pattern of **7i** with H_3R

Identification of *N*-phenyl-3-methoxy-4-pyridinones as orally bioavailable H_3 receptor antagonists and β-amyloid aggregation inhibitors for the treatment of Alzheimer's disease

Minkui Zhang[a#], Li Tang[a,b,#], Liu Jiang[a], Jun Wei[a], Yongzhou Hu[a], Rong Sheng[a*]

a. College of Pharmaceutical Sciences, Zhejiang University, Hangzhou 310058, China;

b.College of Health Science and Environmental Engineering, Shenzhen Technology University, Shenzhen, China

[#]These authors contributed equally to this work.

*Corresponding author

Rong Sheng Tel/Fax: +86-571-8820-8458; E-mail address: *shengr@zju.edu.cn.*

Abstract

Based on our previous work, a series of *N*-phenyl-3-methoxy-4-pyridinone derivatives were designed as orally bioavailable dual functional agents for therapy of Alzheimer's disease, through introducing alkyloxy moiety into 4-pyridinone ring to avoid the possible phase II metabolism of 3-hydroxy-4-pyridinone in lead compound 3-hydroxy-2-methyl-1- (4-(3-(pyrrolidin-1-yl)propoxy)phenyl)-pyridin-4(1*H*)-one **(4)**. *In vitro* studies indicated that most of these compounds exhibit excellent H_3 receptor antagonistic activities and potent self-induced $A\beta_{1-40}/A\beta_{1-42}$ aggregation inhibitory activities. In particular, 3-methoxy-1-(4-(3-(pyrrolidin-1-yl)propoxy)phenyl)-pyridin-4(1H)-one (**7i)** demonstrated IC_{50} value of 0.52 nM in H_3R antagonism and good selectivity over other histamine receptor subtypes. The transmission electron microscopy (TEM) images showed that compound **7i** can inhibit self-mediated

$A\beta_{1-40}$/$A\beta_{1-42}$ aggregation efficiently. As expected, it exhibited desirable pharmacokinetic properties in plasama and good BBB permeability. Furthermore, compound **7i** can efficiently block (R)-α-methylhistamine- induced dipsogenia and reverse scopolamine-induced learning deficits of rats. All above results indicated that compound **7i** was a promising orally bioavailable dual functional agents with potenial use in the treatment of Alzheimer's disease.

Key words: Alzheimer's disease; H_3 receptor antagonists; β-amyloid aggregation inhibition; Dual functional agents.

1. Introduction

Alzheimer's disease (AD) afflicts more than 30 million people worldwide [1]. Although great progress has been made in the treatment of AD in the past few decades, the etiology of this disease remains unclear, and effective therapeutic interventions are still limited except acetylcholinesterase (AChE) inhibitors and *N*-methyl-D-aspartate (NMDA) receptor antagonist memantine [2-5]. AD is a multifactorial disease, and diverse factors, including neurotransmitter system dysfunction, β-amyloid (Aβ) aggregation, τ-protein hyper-phosphorylation, biometal dyshomeostasis, oxidative stress, inflammation, and many more, seem to play significant roles in the progress of AD [6-9]. This multifunctional nature of AD provides the logical foundation for the development of novel drug design strategies, multi-target-directed-ligands (MTDLs), which can simultaneously interfere with different causes of AD and may provide more efficient therapy through a synergistic effect [10-12]. Sodium Oligo-mannurarate (GV-971), a native carbohydrate-based multi-targeting drug has specifically been approved in China for the treatment of mild-to-moderate Alzheimer's disease [13].

The H_3 receptor functions as an auto- and hetero-receptor, negatively regulating the release of histamine and other neurotransmitters, including acetylcholine (ACh), dopamine, noradrenaline, and serotonin [14-17]. The role of AChE inhibitors in the clinic is to disrupt the hydrolysis of ACh in the brain and, thus, palliate memory deficits. The antagonism of the H_3 receptor can increase the concentration of ACh released, as well as other attention-related neurotransmitters in the brain, including serotonin, noradrenaline, and dopamine, and, therefore, may provide a better therapeutic

effect for AD patients. In the past few years, several H_3 receptor antagonists have been approved for clinical trials of various CNS diseases, including CEP-26401 (phase I for cognitive impairment, Cephalon, Figure 1, **1**), MK0249 (phase II for Alzheimer's Disease, Merck, Figure 1, **2**) [18], and Pitolisant, particularly approved by European Medicines Agency (EMA) in 2016 and by Food and Drug Administration (FDA) in 2019 for the treatment of narcolepsy (Figure 1, **3**) [19, 20].

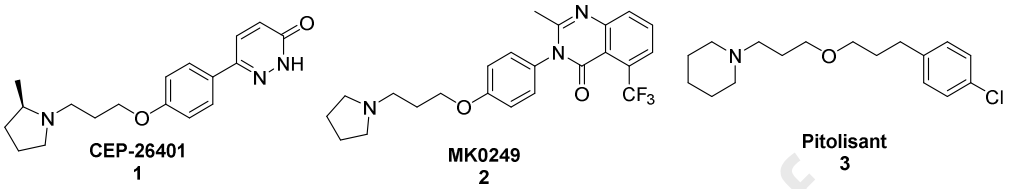

Figure 1. Structures of representative H_3 antagonists

Senile plaques formed by aggregated β-amyloid (Aβ) are the histopathological hallmarks of AD [21-23]. Although the precise neurotic mechanism of aggregated β-amyloid is controversial, numerous investigations have proven that it (both fibril and oligomer aggregated Aβ) is toxic to neuronal cells [24-27]. Therefore, it is necessary to develop Aβ aggregation inhibitors that can benefit AD therapy.

Recently, our group unveiled a series of 1-phenyl-3-hydroxy-4-pyridinone derivatives as potential multi-target agents for AD therapy [28]. Specifically, 3-hydroxy-2-methyl-1-(4-(3-(pyrrolidin-1-yl)propoxy)phenyl)-pyridin-4(1*H*)-one (**4**) demonstrated very potent H_3 receptor antagonistic activity (IC_{50} = 0.32 nM), efficient radical-scavenging effect, excellent copper ion chelating activity, and Aβ aggregation inhibitory activity (Figure 2). However, the oral bioavailability of the compound was relatively low in rats (F = 24 %, see SI), which limited its further development. It's reported that the market chelator Deferiprone (**5**) was metabolized by UDP-glucuronosyl transferases (UGTs) into the corresponding 3-*O*-glucuronide conjugate (**6**) (Figure 4) [29,30]. Based on the structure of **4**, we deduced that the possible reason of low oral bioavailability is the quick phase-II metabolism of the 3-hydroxy-4-pyridinone moiety. Therefore, we try to modify the 3-hydroxyl moiety of the pyridinone ring to block the phase-II metabolism by UGTs, thus to improve the bioavailability of the compound and its permeability through the blood-brain barrier.

Therefore, we present here a series of *N*-phenyl-3-methoxy-4-pyridinones as orally bioavailable H_3 receptor antagonists and β-amyloid aggregation inhibitors. A summary of the drug design strategy is shown in Figure 2, where several regions of the lead compound, **4**, were modified to explore the structure activity relationships (SAR) and find a promising candidate for further development. 1) The modification of substituent groups on the pyridinone ring, the length of the linker, and the cyclic amine moiety to produce compounds **7a-7j.** 2) Replacement of the linear alkyloxy linker with a piperidinyl-ether linker to manufacture compounds **8a-8f**; 3) Replacement of the alkoxy linker with a piperazine-carbonyl or piperazine-sulfonyl linker to furnish compounds **9a-9c** and **10a-10c**.

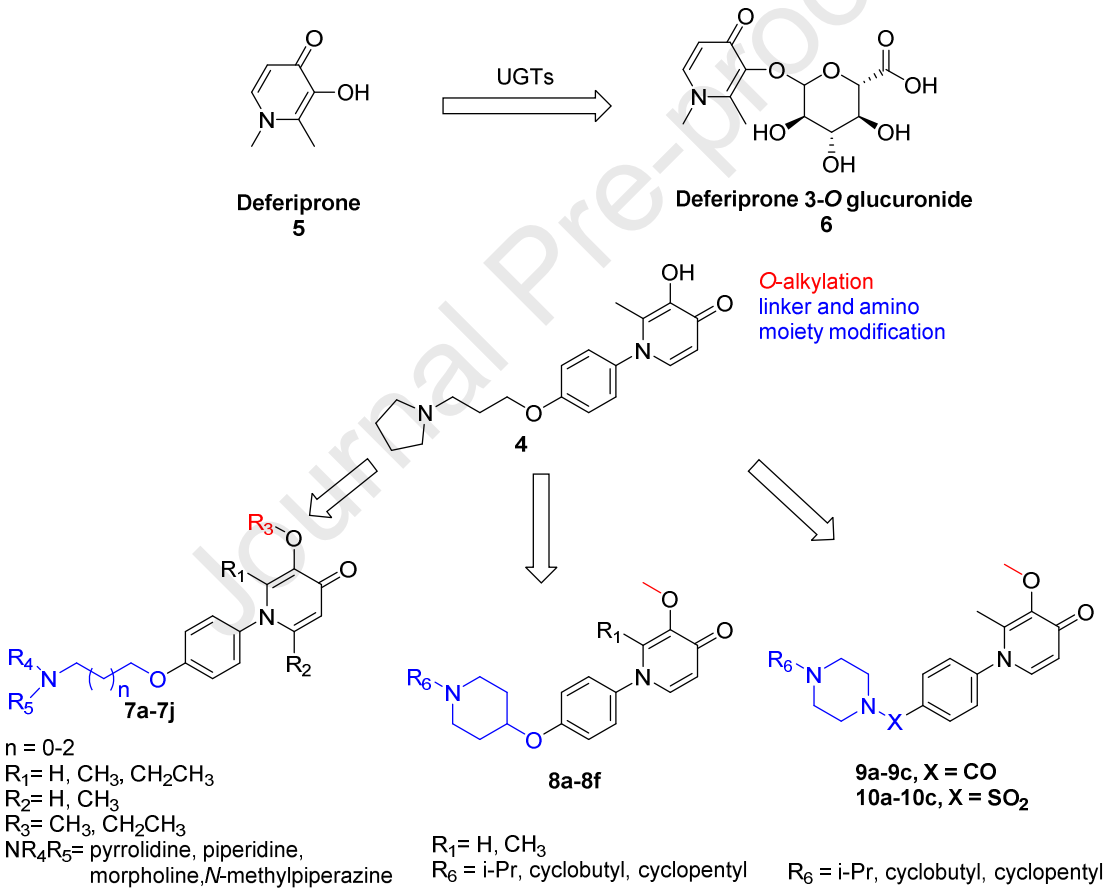

Figure 2. Design strategy for *N*-phenyl-3-methoxy-4-pyridinone derivatives

2. Results and discussion

2.1 Chemistry

The synthesis of *N*-phenyl-3-methoxy-4-pyridinone derivatives **7a-7j** with a linear linker is described in **Scheme 1**. Starting materials, compounds **11a-11e,** were prepared as described

previously [28]. **11a-11e** reacted with 4-aminophenol to form *N*-phenolpyridinone **12a-12e** under microwave conditions. **12a-12e** were then alkylated with α,ω-dihaloalkane in the presence of K_2CO_3 to yield compounds **13a-13g**, which were condensed with various secondary amines to obtain target compounds **7a-7j**.

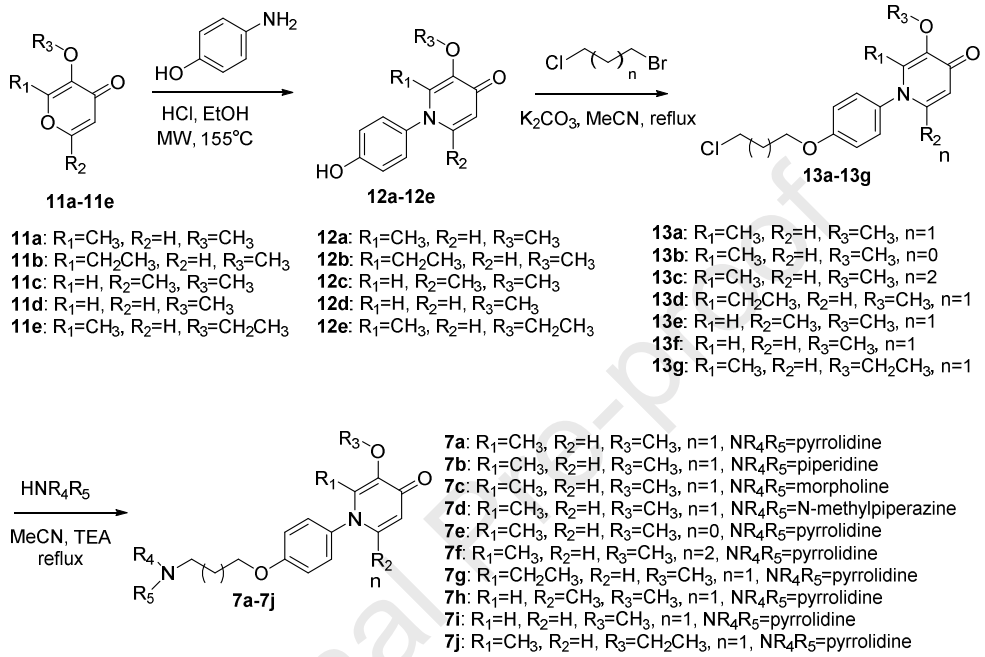

Scheme 1. Synthetic route to **7a-7j** with linear linker

The synthesis of **8a-8f** with a 4-piperidinyl-ether linker is described in Scheme **2**. 4-fluoronitrobenzene, **14,** reacted with *N*-Boc-4-hydroxypiperidine to yield phenoxy piperidine derivative **15**, followed by the deprotection of Boc, reductive amination, and the reduction of the nitro-group to produce aniline derivatives **18a-18c**. **18a-18c** then reacted with 3-alkoxy-4-pyrone to create target compounds **8a-8f**.

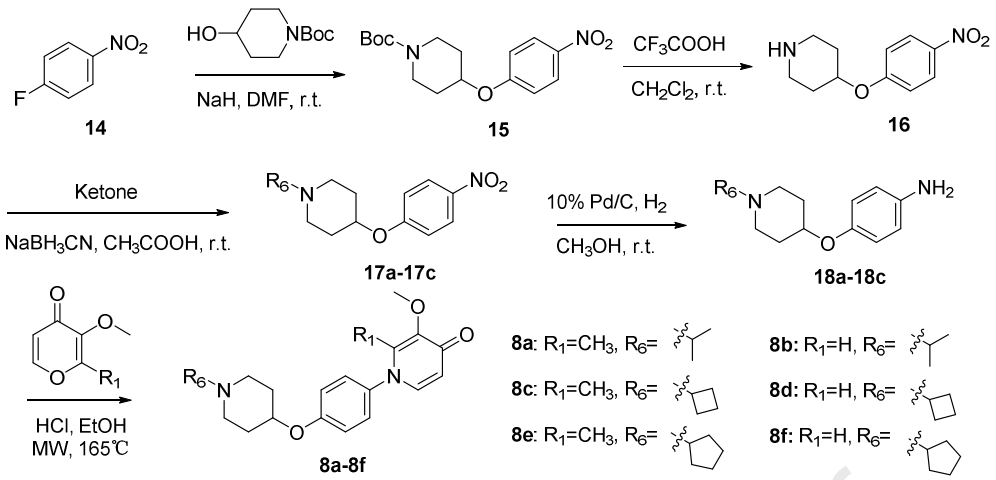

Scheme 2. Synthetic route to **8a-8f** with 4-piperidinyl-ether linker

The synthesis of **9a-9c** with a piperazine-carbonyl linker is described in Scheme **3**. Compound **11a** reacted with 4-aminobenzoic acid in a sealed tube to give rise to intermediate **19**. **19** was condensed with *N*-Boc piperazine, after which Boc was deprotected to obtain key intermediate **21**. **21** was subsequently subjected to reductive amination with various ketones to produce target compounds **9a**-**9c**.

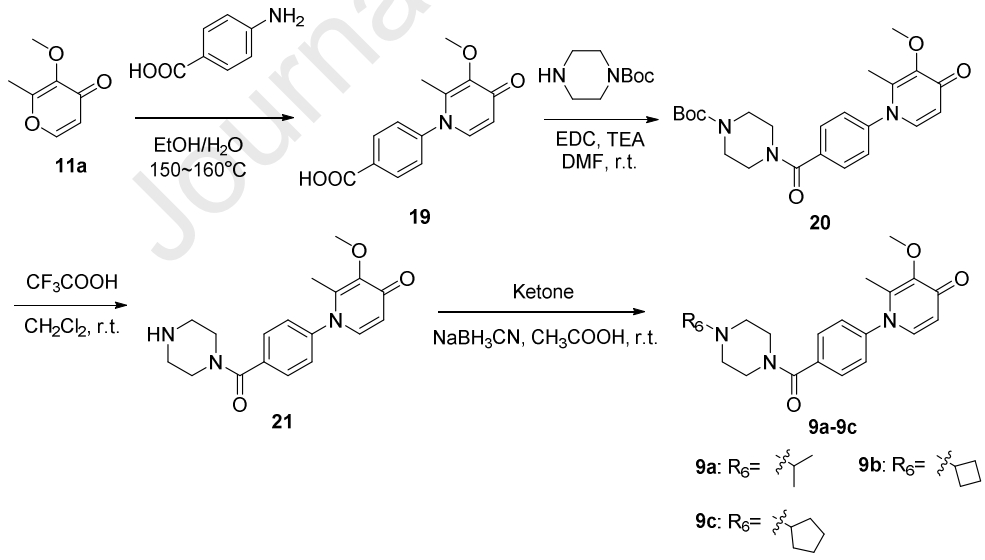

Scheme 3. Synthetic route to **9a-9c** with piperazine-carbonyl linker

The synthesis of derivatives **10a-10c** with a piperazine-sulfonyl linker is described in Scheme **4.** 4-nitrobenzenesulfonyl chloride, **22,** was condensed with *N*-Boc-piperazine, followed by the deprotection of Boc to obtain intermediate **24**. **24** was reductively aminated with different ketones

to yield intermediates **25a-25c**, whose nitro moieties were reduced by catalytic hydrogenation to create aniline derivatives **26a-26c**. **26a-26c** were eventually condensed with 3-methyl-4-pyrone, **11a,** to furnish target compounds **10a-10c.**

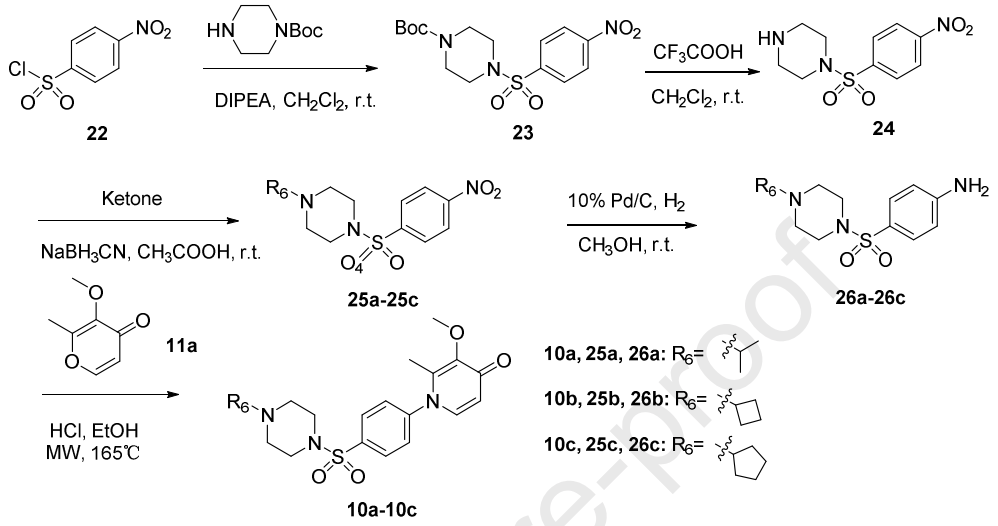

Scheme 4. Synthetic route to **10a-10c** with piperazine-sulfonyl linker

2.2 H_3R antagonistic and $A\beta_{1-40}/A\beta_{1-42}$ aggregation inhibitory activity evaluation

The H_3 receptor antagonistic activities of these *N*-phenyl-3-methoxy-4-pyridinones were determined using the cAMP-response elements (CREs)-driven luciferase assay in hH_3 receptor-expressed HEK-293 cell lines, and their $A\beta_{1-40}/A\beta_{1-42}$ aggregation inhibitory activities were evaluated using the thioflavin T fluorescence assay [28].

The biological activities of these target compounds are shown in Table **1**. Many of the *N*-Phenyl-3-methoxy-4-pyridinone derivatives demonstrated potent hH_3R antagonistic activities and efficient $A\beta_{1-40}/A\beta_{1-42}$ aggregation inhibitory activities. 13 compounds (**7a**, **7b**, **7f-7j**, **8a-8f**) showed nanomolar or subnanomolar IC_{50} values against the H_3 receptor. In addition, 20 μM of each of 18 compounds (**7a-7j**, **8a-8f**, **10b**, **10c**) exhibited 50.7-80.5% inhibition rates on $A\beta_{1-40}$ aggregation, compared with the 54.8% inhibition rate of curcumin, and 12 compounds (**7a**, **7c-7e**, **7g-7j**, **8a**, **9a**, **10a**, **10b**) exhibited 50.9-67.5% inhibition rates on $A\beta_{1-42}$ aggregation, compared with the 65.7% inhibition rate of curcumin. Some compounds showed significantly different activities on $A\beta_{1-40}$ and $A\beta_{1-42}$, suggesting that there may be different modes of action between the compounds and $A\beta_{1-40}/A\beta_{1-42}$.

The changes in the terminal cyclic amine group affected the H_3 antagonistic activities of target compounds. The pyrrolidine and piperidine derivatives, **7a** and **7b**, respectively, displayed similar activities, while the morpholine and methyl piperazine analogs, **7c** and **7d**, respectively, showed a drastic loss of activity in H_3 antagonism, which is consistent with our previous results [28]. However, these changes did not affect the $A\beta_{1-40}/A\beta_{1-42}$ aggregation inhibitory activities of these derivatives significantly.

7f, with four carbon length linkers, retained its hH_3R activity and $A\beta_{1-40}$ aggregation inhibitory activity but lost its $A\beta_{1-42}$ aggregation inhibitory activity, whereas, **7e,** with a short length linker, almost lost its hH_3R inhibitory effect and bore a slight change in its $A\beta_{1-40}$ and $A\beta_{1-42}$ aggregation inhibitory activities.

The changes in the alkyl group and their substitution positions on the 4-pyridinone ring resulted in the production of compounds **7g-7j**, all of which demonstrated potent H_3 antagonistic activities, with IC_{50} values ranging from 0.52 to 7.97 nM, and good $A\beta_{1-40}/A\beta_{1-42}$ inhibitory effects, indicating that minor modifications on the pyridinone ring do not affect H_3 antagonism or $A\beta_{1-40}/A\beta_{1-42}$ inhibition. Compound **7i** was the most potent hH_3R antagonist, with a IC_{50} value of 0.52 nM, a $A\beta_{1-40}$ inhibitory rate of 56.0% and a $A\beta_{1-42}$ inhibitory rate of 63.4% at 20 μM.

Replacing the linear alkyoxy linker of **7a** with 4-piperidinyl-ether, piperazine-carbonyl, or piperazine-sulfonyl resulted in the creation of the other three series of compounds **8a-8f, 9a-9c,** and **10a-10c**. Compounds **8a-8f** retained potent H_3R antagonistic activities, with IC_{50} values that ranged from 0.46 to 8.92 nM, and good $A\beta_{1-40}$ inhibitory activities (50.7-59.6% inhibition at 20 μM). In contrast, the other two serial compounds **9a-9c** and **10a-10c** only showed moderate H_3R antagonistic activities, with IC_{50} values that ranged from 22.11 to 350.5 nM, and decreased $A\beta_{1-40}$ inhibitory activities (21.2-54.6%). Meanwhile, almost all of these compounds exhibited decreased $A\beta_{1-42}$ inhibitory activities, except isopropyl substituted compounds (**8a**, **9a**, **10a**). These findings suggest that the linkers of target compounds play vital roles in H_3 antagonism.

Table 1. Biological activities of N-phenyl-3-methoxy-4-pyridinone derivatives [a]

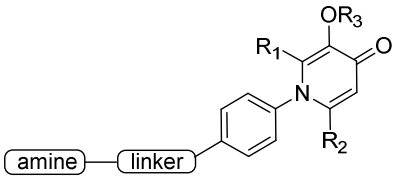

Cpd.	amine	linker	R_1	R_2	R_3	hH_3R IC_{50} (nM)	Inhibition of Aβ aggregation (%)[b]	
							$Aβ_{1-40}$	$Aβ_{1-42}$
7a		-$O(CH_2)_3$-	Me	H	Me	6.53±0.84	80.5±6.2	52.4±3.5
7b		-$O(CH_2)_3$-	Me	H	Me	5.82±0.23	80.4±7.9	45.1±7.5
7c		-$O(CH_2)_3$-	Me	H	Me	107.8±12.5	69.8±9.5	56.6±2.5
7d		-$O(CH_2)_3$-	Me	H	Me	167.4±26.8	76.1±8.8	67.0±10.6
7e		-$O(CH_2)_2$-	Me	H	Me	1787.1±104	51.6±7.4	59.1±1.9
7f		-$O(CH_2)_4$-	Me	H	Me	4.33±0.30	77.3±5.1	26.9±4.2
7g		-$O(CH_2)_3$-	Et	H	Me	1.11±0.08	64.9±2.9	62.4±3.2
7h		-$O(CH_2)_3$-	H	Me	Me	1.94±0.49	60.1±6.8	55.2±2.7
7i		-$O(CH_2)_3$-	H	H	Me	0.52±0.07	56.0±8.4	63.4±9.9
7j		-$O(CH_2)_3$-	Me	H	Et	7.97±0.88	52.7±3.7	67.5±1.9
8a	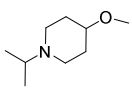		Me	H	Me	8.92±0.54	54.4±3.1	63.5±5.3
8b			H	H	Me	1.67±0.14	58.5±6.4	41.4±6.1
8c	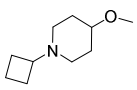		Me	H	Me	2.43±0.18	59.6±4.9	7.5±3.4
8d			H	H	Me	0.74±0.59	52.5±7.2	9.3±1.7
8e	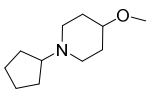		Me	H	Me	1.39±0.37	57.9±2.8	1.5±2.5
8f			H	H	Me	0.46±0.06	50.7±4.9	N
9a	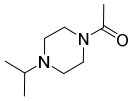		Me	H	Me	350.5±29.8	28.5±7.9	50.9±1.6
9b	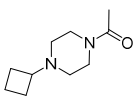		Me	H	Me	68.30±0.06	43.6±6.7	44.3±6.1

9c	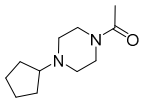	Me	H	Me	49.04±2.81	49.0±3.4	23.9±7.9
10a	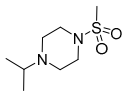	Me	H	Me	385.3±25.8	21.2±4.1	64.0±4.1
10b	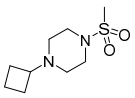	Me	H	Me	35.81±2.14	51.5±6.9	54.4±8.9
10c	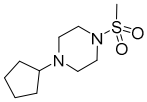	Me	H	Me	22.11±3.56	54.6±5.0	N
	Clobenpropit				1.15±0.16	/	/
	Curumin				/	54.8±6.5	65.7±5.3

[a] The values are expressed as the Mean±SD of three independent measurements.

[b] 20 μM of compounds and 25 μM of $A\beta_{1-40}$ or $A\beta_{1-42}$ were used.

[c] "N" means not determined.

2.3 Selectivity of the histamine receptor subtype

Based on hH_3R antagonistic activities and $A\beta_{1-40}/A\beta_{1-42}$ aggregation inhibitory activities, the most promising compound, **7i,** was selected for further investigation. The antagonistic activities of **7i** on three histamine receptor subtypes (H_1R, H_2R, and H_4R) were evaluated using the CRE-luciferase assay as previous described [28]. Table **2** reveals that compound **7i** had no antagonistic activity against H_1R, H_2R, or H_4R, indicating the high selectivity of **7i** for H_3 receptors.

2.4 hERG channel inhibition

The development of many reported highly potent H_3 antagonists have been stopped at the preclinical trial stage because of their hERG channel inhibitory activities that is closely associated with prolonging the QT interval [31]. As shown in Table 2, compound **7i** (3.0 μM) only had a 6.3% inhibitory effect on the hERG channel in the patch-clamp assay, indicating that it has a low risk of prolonging the QT interval.

Table 2. Histamine Receptor Subtype Selectivity and hERG Inhibition of Compound **7i**.

Compound	hH_1R (IC_{50}, μM)	hH_2R (IC_{50}, μM)	hH_4R (IC_{50}, μM)	hERG inhibition
7i (3.0 μM)	>10	>10	>10	6.3% ± 1.5%
Cisapride (30 nM)	/	/	/	44.1% ± 1.5%

*2.5 Study of the molecular docking of **7i** with the H_3 receptor*

To assess the binding modes of this class of 1-phenyl-4-pyridinone derivatives with H_3R, compound **7i** was selected for docking studies using previously established H_3 receptor homology model based on the H_1 receptor crystal structure (PDB ID: 3RZE) [32]. The result showed that compound **7i** fitted well in the hydrophobic pocket formed by the TMs 3-5-6 region and three hydrogen bonds between the amino acid residues of the H_3 receptor formed. The methoxy moiety of pyridinone of **7i** formed a hydrogen bond with the OH group of Thr201, the alkoxy linker formed another hydrogen bond with the oxygen of the phenol moiety of Tyr 374, and the protonated nitrogen of the pyrrolidine moiety formed the third hydrogen bond with the carboxylic acid of critical amino acid Asp114 (Figure 3). Additionally, the phenyl ring of **7i** interacted with the aromatic ring of Tyr 115 in a π−π stacking mode.

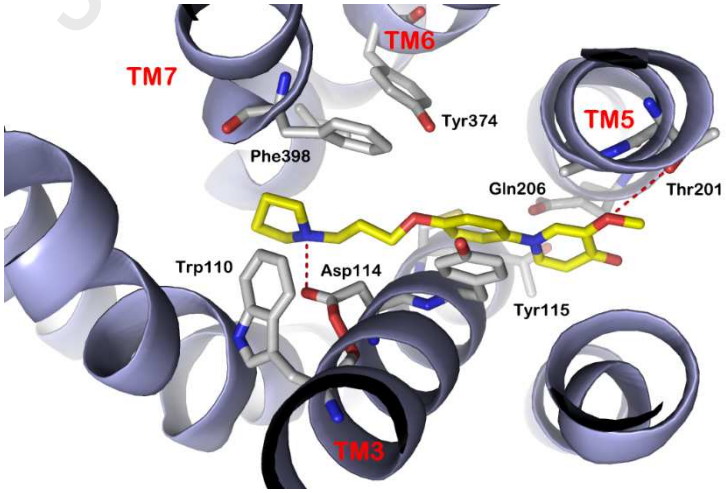

Figure 3. The binding pattern of **7i** with H_3R homology model.

*2.6 The inhibition of Self-induced $A\beta_{1\text{-}40}$ and $A\beta_{1\text{-}42}$ aggregation by **7i***

Besides using the ThT binding assay, the effect of **7i** on self-induced *Aβ$_{1-40}$ and Aβ$_{1-42}$* aggregation was monitored using transmission electron microscopy (TEM) as described previously [28]. As shown in Figure **4**, after 24 h of incubation at 37 °C, Aβ$_{1-42}$ self-aggregated into amyloid fibrils, while Aβ$_{1-40}$ self-aggregated into amyloid fibrils as well as plaque-like aggregates. However, when curcumin or **7i** was added (Figure **4c**, **4d**) under identical conditions only very few Aβ$_{1-40}$ or Aβ$_{1-42}$ fibrils were observed in TEM.

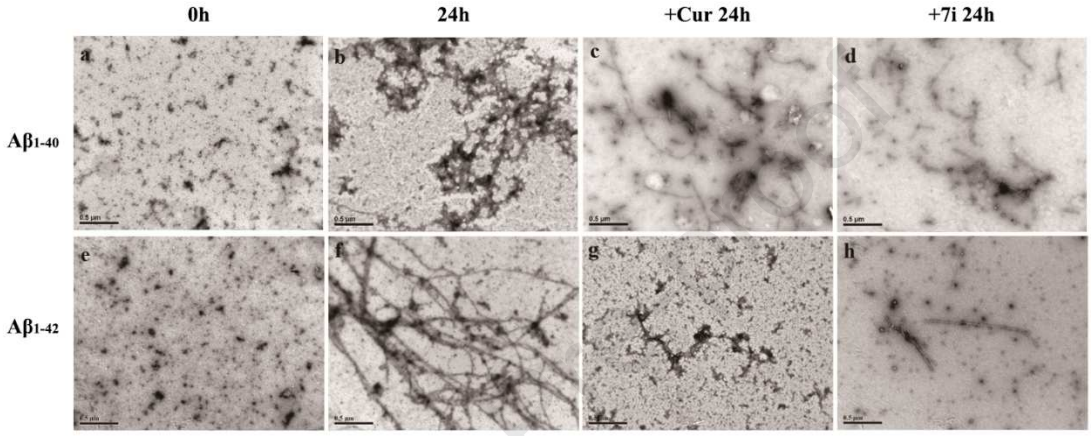

Figure 4. TEM images of samples of Aβ$_{1-40}$ and Aβ$_{1-42}$. ([Aβ] = 25 μM, 37°C, constant agitation).

(a) Aβ$_{1-40}$ alone, 0h (b) Aβ$_{1-40}$ alone, 24h (c) Aβ$_{1-40}$+**curcumin**, 24h (d) Aβ$_{1-40}$ +**7i**, 24h

(e) Aβ$_{1-42}$ alone, 0h (f) Aβ$_{1-42}$ alone, 24h (g) Aβ$_{1-42}$+**curcumin**, 24h (h) Aβ$_{1-42}$ +**7i**, 24h

*2.7 Disaggregation of Self-induced Aβ$_{1-40}$ and Aβ$_{1-42}$ aggregation by **7i***

Self-induced Aβ$_{1-40}$ and Aβ$_{1-42}$ aggregation fibrils were incubated with **7i** to investigate the disaggregation activity of **7i**. Fresh Aβ$_{1-40}$/Aβ$_{1-42}$ was incubated for 24 h at 37 °C to yield Aβ$_{1-40}$/Aβ$_{1-42}$ fibrils. **7i** or curcumin was then added to the fibrils and incubated for another 24 h under the same condition. Figure 5 shows that **7i** disassembled the well-formed Aβ$_{1-40}$/Aβ$_{1-42}$ fibrils efficiently, as did curcumin.

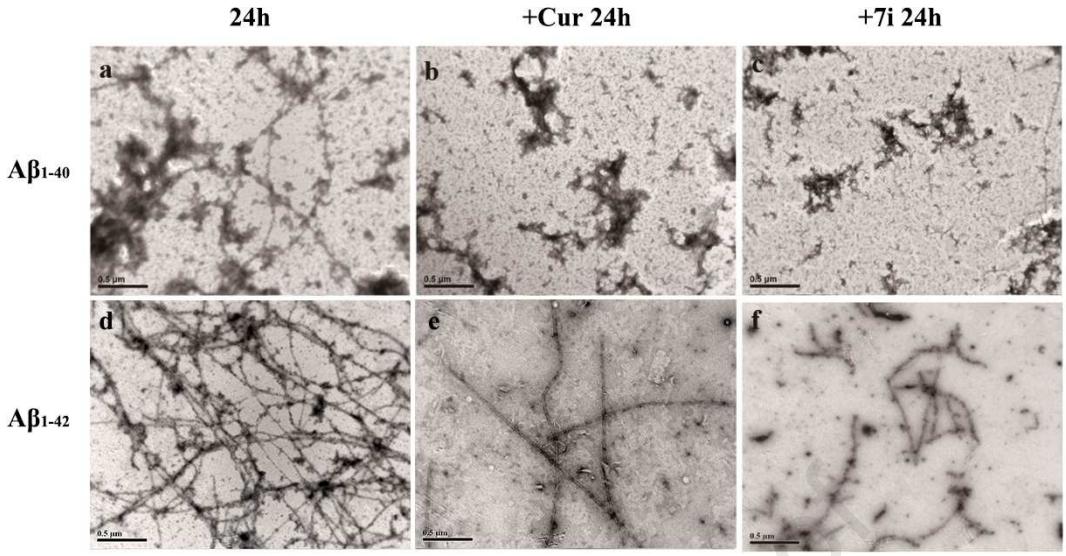

Figure 5. TEM images of disaggregation experiments on $A\beta_{1-40}$ and $A\beta_{1-42}$ fibers.

([Aβ] = 25 μM, 37°C, constant agitation,24h).

(a) $A\beta_{1-40}$ alone. (b) $A\beta_{1-40}$+curcumin. (c) $A\beta_{1-40}$ +**7i**.

(d) $A\beta_{1-42}$ alone. (e) $A\beta_{1-42}$+curcumin. (f) $A\beta_{1-42}$ +**7i.**

*2.8 The molecular docking of **7i** with $A\beta_{1-40}$ and $A\beta_{1-42}$*

To elucidate the binding modes of compound **7i** with monomeric $A\beta_{1-40}$ and $A\beta_{1-42}$, molecular docking was performed using Accelrys Discovery Studio 2.0, and the crystal structure of $A\beta_{1-40}$ and $A\beta_{1-42}$ (PDB code: 1BA4, 1IYT) was employed [33].

As shown in Figure 6, compound **7i** bound slightly differently with $A\beta_{1-40}$ and $A\beta_{1-42}$. **7i** was located in the middle part of $A\beta_{1-40}$ and interacted with residues of Asp23 and Lys28. A hydrogen bond was formed between the carbonyl moiety of 4-pyridinone and the NH group of Lys28, and salt bridges were erected between the basic pyrrolidine moiety of **7i** and Asp23. The binding mode of **7i** with $A\beta_{1-42}$ was similar to that of the lead compound **4**, it bound to the molecular surface of the C-terminus of the peptide chain to form hydrogen bonds and salt bridges with Lys28 and Ala42, respectively. These results are consistent with the finding (Table 1) that **7i** interact with $A\beta_{1-40}$ and $A\beta_{1-42}$ in a different way.

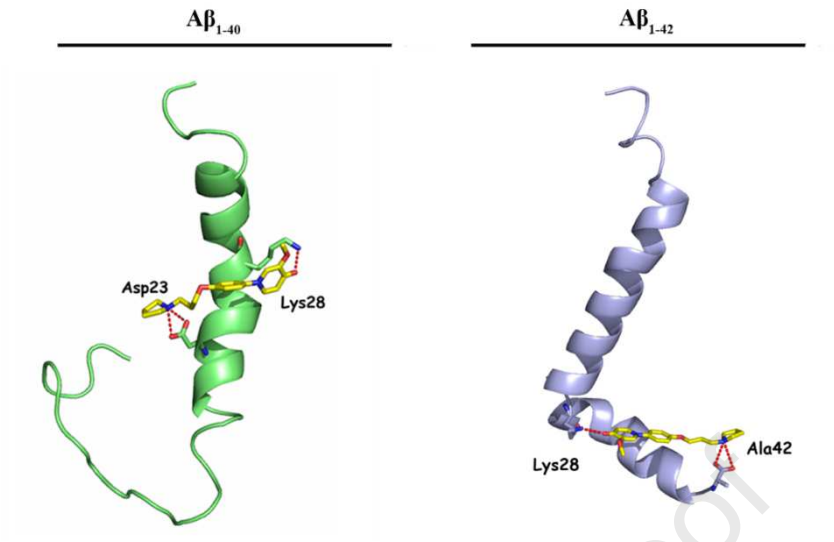

Figure 6. The binding pattern of **7i** with monomeric $A\beta_{1-40}$ and $A\beta_{1-42}$

2.9 In vivo pharmacokinetic study

We investigated the *in vivo* preliminary pharmacokinetic properties of compound **7i** in rats (Figure 7, Table 3). After the intravenous administration of 2.0 mg/kg and intragastric administration of 5.0 mg/kg of **7i** to rats, blood exposure to the compound (AUC_{0-t}) reached 1412.5 ng•h/mL and 1266.4 ng•h/mL, respectively, with corresponding elimination half-lives of 1.59 hours and 4.64 hours. The oral bioavailability of **7i** was 47.9%. Compared to compound **4** (p.o. 10 mg/kg; AUC_{0-t} 1035.7 ng•h/mL; F value of 24.0%, Supplementary Table S1), **7i** had significantly improved oral exposure and bioavailability.

Additionally, brain exposure (AUC_{0-t}) to **7i** was 359.6 ng•h/mL and 277.2 ng•h/mL after intravenous administration of 2.0 mg/kg and intragastric administration of 5.0 mg/kg, respectively, with corresponding B/P values of 0.40 and 0.44.

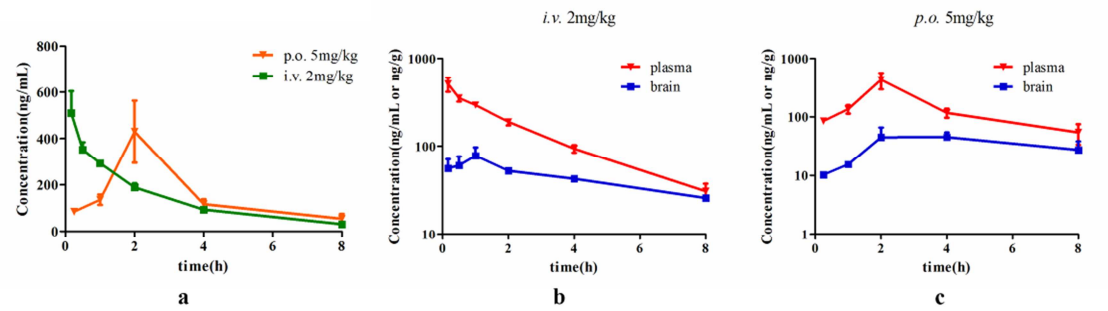

Figure 7. The *in vivo* PK profile of **7i**

Table 3. Pharmacokinetic Properties of Compound **7i**

	***i.v.* (2.0 mg/kg)**		***p.o.* (5.0 mg/kg)**	
	plasma	**brain**	**plasma**	**brain**
AUC_{0-t} (ng·h/mL)	1412.5	359.6	1266.4	277.2
$AUC_{0-\infty}$ (ng·h/mL)	1412.6	570.8	1693.4	737.8
$T_{1/2}$ (h)	1.59	5.64	4.64	3.77
Cl (L/h/kg)	1.43	3.54	3.26	6.89
V_d (L/kg)	3.27	28.5	18.9	36.5
T_{max} (h)	0.16	1.00	2.00	3.33
C_{max} (ng/mL)	510.5	77.8	429.6	49.9
B/P	0.40		0.44	
F%	-		47.9	

2.10 Dipsogenia model

The excellent H_3 antagonistic activity *in vitro* and good PK profile of **7i** prompted us to carry out *in vivo* pharmacological experiments. The effect of compound **7i** on the H_3 receptor agonist-induced dipsogenia model (SD rats) was tested at different times [34]. As shown in Figure **8** and Table **S2**, rats that were given (R)-α-Methylhistamine (2.5 mg/kg s.c.) for 2 h consumed about 2.5-fold more water than vehicle control. Conversely, the three groups of rats that received different doses of compound **7i** (0.3 mg/kg, 1.0 mg/kg, and 3.0 mg/kg) consumed less water in a dose-dependent manner, with an effective concentration of 0.3 mg/kg. These results demonstrate that **7i** can exert the function of an H_3 receptor antagonist *in vivo*.

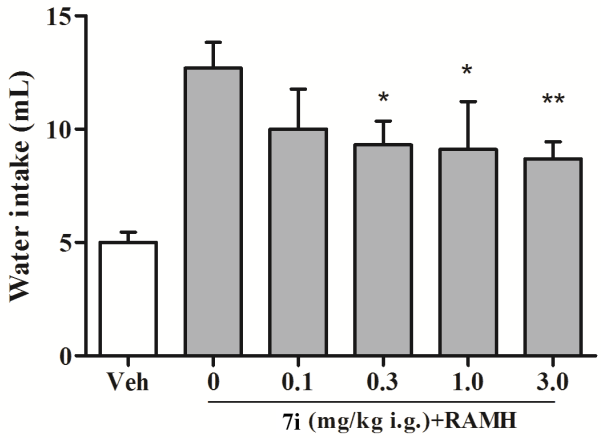

Figure 8. Evaluation of **7i** in (R)-α-methylhistamine-induced dipsogenia model in 2 hours (rats, n = 8 per group). White bar shows the vehicle model, black bars shows groups taken (R)-α-methylhistamine and different dose of **7i** (*, $p<0.05$; **, $p<0.01$ compared with (R)-α-methylhistamine alone group).

2.11 Morris Water Maze Testing

To further investigate the effect of **7i** on an AD model, we performed the Morris water maze of scopolamine-induced spatial learning and memory deficits study in rats [35]. The difference in the latency time taken by rats to find the platform was used as the evaluation parameter. Results indicate that the anticholinergic agent, scopolamine, caused a significant learning impairment in rats (Figure **9,** Table **S3**), while pretreatment with **7i** (1.0 or 3.0 mg/kg for 2 h before each training session) significantly reversed these memory deficits, confirming the fact that H_3 antagonist **7i** could improve the cholinergic function of rats.

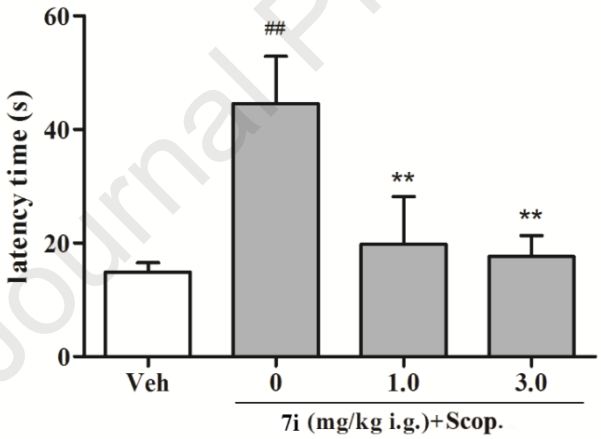

Figure 9. Evaluation of compound **7i** on Morris water maze. ($^{##}$, $p<0.05$ versus vehicle; **, $p<0.01$ versus scopolamine, n = 8 per group.)

3. Conclusion

In summary, to avoid the possible phase II metabolism of lead compound **4**, the 3-hydroxy-4-pyridinone moiety was changed to alkyloxy moiety and a series of N-phenyl-3-methoxy-4-pyridinone derivatives were synthesized and evaluated as orally bioavailable H_3 receptor antagonists with β-amyloid aggregation inhibitory activities. Further biological evaluations on the most promising compound **7i**, indicate that it possesses a potent and high selective H_3 receptor antagonistic activity *in vitro* and *in vivo*, a good PK profile

accompanied with good BBB permeability and low hERG inhibition risk. These results suggest that **7i** has therapeutic potential as a novel multi-target agent for the treatment of Alzheimer's disease.

Acknowledgments

This study was supported by the National Natural Science Foundation of China (21172193) and Zhejiang Provincial Natural Foundation of China (No.R2110297). We thank Jianyang Pan (Research and Service Center, College of Pharmaceutical Sciences, Zhejiang University) for performing NMR spectrometry for structure elucidation

4. Experimental section

4.1 Biology

General procedure of biological evaluation is presented in Supplementary Information.

4.2 Chemistry

General Methods. All Reagents and solvents were purchased from common commercial of analytical grade. ^{1}H NMR were recorded on a BRUKER AVANCE III 500 M spectrometer, ^{13}C NMR were recorded on a 125 MHz spectrometer (chemical shifts are given in ppm relative to TMS as internal standard). Mass spectra (ESI-MS) were performed on an FINNIGAN LCQ-DECAXP spectrometer.

General Synthetic Procedure for compound 12a-12e

A mixture of compound **11a-11e** (2.0 mmol), aminophenol (4.4 mmol), 2.5 mL diluted HCl solution and 2.0 mL ethanol was placed in a MW tube (10mL) containing a magnetic stirring bar. The reaction tube was sealed and irradiated in the cavity of a microwave apparatus at 155 ℃ for 25 minutes. After completion of the reaction, the tube was removed, cooled to ambient temperature, and the precipitate was filtered and rinsed with hot water to afford **12a-12e.**

3-Methoxy-1-(4-hydroxyphenyl)-2-methylpyridin-4(1H)-one (12a)

Pale-yellow solid, yield: 74%. ^{1}H NMR (500 MHz, DMSO-d_6): δ 10.03 (s, 1H), 7.53 (d, *J* = 7.5 Hz, 1H), 7.25 (d, *J* = 9.0 Hz, 2H), 6.89 (d, *J* = 9.0 Hz, 2H), 6.16 (d, *J* = 7.5 Hz, 1H), 3.73 (s, 3H), 1.96 (s, 3H). ESI-MS: *m/z*=232 $[M+H]^+$.

3-Methoxy-1-(4-hydroxyphenyl)-2-ethylpyridin-4(1H)-one (12b)

Yellow solid, yield: 63%. ^{1}H NMR (500 MHz, DMSO-d_6): δ 10.02 (s, 1H), 7.48 (d, *J* = 7.5 Hz, 1H), 7.27 (d, *J* = 9.0 Hz, 2H), 6.89 (d, *J* = 9.0 Hz, 2H), 6.16 (d, *J* = 7.5 Hz, 1H), 3.80 (s, 3H), 2.39 (q, *J* = 6.0 Hz, 2H), 0.91 (q, *J* = 6.0 Hz, 3H). ESI-MS: *m/z*=246 $[M+H]^+$.

5-Methoxy-1-(4-hydroxyphenyl)-2-methylpyridin-4(1H)-one (12c)

Yellow soild, yield: 73%, ^{1}H NMR (400 MHz, DMSO-d_6): δ 10.00 (s, 1H), 7.25-7.23 (m, 3H), 6.89 (d, *J* = 8.4 Hz, 2H), 6.14 (s, 1H), 3.62 (s, 3H), 1.93 (s, 3H). ESI-MS: *m/z*=232 $[M+H]^+$.

3-Methoxy-1-(4-hydroxyphenyl)pyridin-4(1H)-one (12d)

Yellow soild, yield: 67%, ^{1}H NMR (400 MHz, DMSO-d_6): δ 9.88 (s, 1H), 7.77 (d, *J* = 7.2 Hz, 1H), 7.57 (s, 1H); 7.40 (d, *J* = 8.4 Hz, 2H), 6.90 (d, *J* = 8.4 Hz, 2H), 6.21 (d, *J* = 7.2 Hz, 1H), 3.71 (s, 3H). ESI-MS: *m/z*=218 $[M+H]^+$.

3-Ethoxy-1-(4-hydroxyphenyl)-2-methylpyridin-4(1H)-one (12e)

Yellow soild, yield 71%. ^{1}H NMR (500 MHz, DMSO-d_6): δ 10.03 (s, 1H), 7.52 (d, *J* = 7.5 Hz, 1H), 7.24 (d, *J* = 9.0 Hz, 2H), 6.88 (d, *J* = 9.0 Hz, 2H), 6.16 (d, *J* = 7.5 Hz, 1H), 4.07 (q, *J* = 7.0 Hz, 2H), 1.97 (s, 3H), 1.24 (t, *J* = 7.0 Hz, 3H). ESI-MS: *m/z*=246 $[M+H]^+$.

General Synthetic Procedure for compound 13a-13g

A mixture of compound **12a-12e** (5.0 mmol), K_2CO_3 (1.38g, 10.0 mmol), and 1-bromo-3-chloropropane (or 1-bromo-2-chloroethane, or 1-bromo-4-chlorobutane, 1.0 mL, 10.0 mmol) was refluxed in 25 mL acetonitrile for 6-8 hours. The mixture was cooled to ambient temperature, filtered, washed with acetonitrile and concentrated to dryness. The crude product was purified by silica gel chromatography to give pure **13a-13g**.

3-Methoxy-1-(4-(3-chloropropoxy)phenyl)-2-methylpyridin-4(1H)-one (13a)

Yellow soild, yield 80%. ^{1}H NMR (500 MHz, $CDCl_3$): δ 7.20 (d, *J* = 7.5 Hz, 1H), 7.12 (d, *J* = 9.0 Hz, 2H), 6.95 (d, *J* = 9.0 Hz, 2H), 6.42 (d, *J* = 7.5 Hz, 1H), 4.13 (t, J = 6.0 Hz, 2H), 3.86 (s, 3H), 3.72 (t, *J* = 6.0 Hz, 2H), 2.24-2.19 (m, 2H), 2.00 (s, 3H). ESI-MS: *m/z*=308 $[M+H]^+$.

3-Methoxy-1-(4-(2-chloroethoxy)phenyl)-2-methylpyridin-4(1H)-one (13b)

Pale-yellow soild, yield 59%. ^{1}H NMR (500 MHz, $CDCl_3$): δ 7.26 (d, *J* = 7.5 Hz, 1H), 7.20 (d, *J* = 9.0 Hz, 2H), 7.03 (d, *J* = 9.0 Hz, 2H), 6.47 (d, *J* = 7.5 Hz, 1H), 4.29 (t, J = 6.0 Hz, 2H), 3.90 (s, 3H), 3.86(t, *J* = 6.0 Hz, 2H), 2.05 (s, 3H). ESI-MS: *m/z*=294 $[M+H]^+$.

3-Methoxy-1-(4-(4-chlorobutoxy)phenyl)-2-methylpyridin-4(1H)-one (13c)

Pale-yellow soild, yield 59%. ^{1}H NMR (500 MHz, $CDCl_3$): δ 7.29 (d, *J* = 7.5 Hz, 1H), 7.20 (d, *J* = 9.0 Hz, 2H), 7.00 (d, *J* = 9.0 Hz, 2H), 6.54 (d, *J* = 7.5 Hz, 1H), 4.06 (t, J = 6.0 Hz, 2H), 3.92 (s, 3H), 3.65(t, *J* = 6.0 Hz, 2H), 2.07 (s, 3H), 2.00-1.98 (m, 4H). ESI-MS: *m/z*=322 $[M+H]^+$.

3-Methoxy-1-(4-(3-chloropropoxy)phenyl)-2-ethylpyridin -4(1H)-one (13d)

Pale-yellow soild, yield 76%. ^{1}H NMR (500 MHz, $CDCl_3$): δ 7.16-7.13 (m, 3H), 6.94 (d, *J* = 9.0 Hz, 2H), 6.40 (d, *J* = 7.5 Hz, 1H), 4.13 (t, *J* = 6.0 Hz, 2H), 3.90 (s, 3H), 3.72 (t, *J* = 6.0 Hz, 2H), 2.44 (q, *J* = 7.5 Hz, 2H), 2.24-2.19 (m, 2H), 0.94 (t, *J* = 7.5 Hz, 3H). ESI-MS: *m/z*=322 $[M+H]^+$.

5-Methoxy-1-(4-(3-chloropropoxy)phenyl)-2-methylpyridin-4(1H)-one (13e)

Pale-yellow soild, yield: 85%, ^{1}H NMR (500 MHz, $CDCl_3$): δ 7.23 (d, *J* = 9.0 Hz, 2H), 7.04 (d, *J* = 9.0 Hz, 2H), 6.98 (s, 1H), 6.44 (s, 1H), 4.20 (t, *J* = 6.0 Hz, 2H), 3.79 (t, *J* = 6.0 Hz, 2H), 3.76 (s, 3H), 2.31-2.26 (m, 2H), 2.02 (s, 3H). ESI-MS: *m/z*=308 $[M+H]^+$.

3-Methoxy-1-(4-(3-chloropropoxy)phenyl)- pyridin-4(1H)-one (13f)

Pale-yellow soild, yield 66%. ^{1}H NMR (500 MHz, $CDCl_3$): δ 7.57-7.56 (m, 1H), 7.38 (d, *J* = 9.0 Hz, 2H), 7.32-7.31 (m, 1H), 7.03 (d, *J* = 9.0 Hz, 2H), 6.57 (d, *J* = 7.0 Hz, 1H), 4.18 (t, *J* = 6.0 Hz, 2H), 3.88 (s, 3H), 3.78 (t, *J* = 6.0 Hz, 2H), 2.33-2.25 (m, 2H). ESI-MS: *m/z*=294 $[M+H]^+$.

3-Ethoxy-1-(4-(3-chloropropoxy)phenyl)-2-methylpyridin-4(1H)-one (13g)

Pale-yellow soild, yield 77%. ^{1}H NMR (500 MHz, $CDCl_3$): δ 7.19 (d, *J* = 7.5 Hz, 1H), 7.12 (d, *J* = 9.0 Hz, 2H), 6.95 (d, *J* = 9.0 Hz, 2H), 6.38 (d, *J* = 7.5 Hz, 1H), 4.18 (q, *J* = 7.0 Hz, 2H), 4.12 (t, *J* = 6.0 Hz, 2H), 3.72 (t, *J* = 6.0 Hz, 2H), 2.24-2.19 (m, 2H), 2.00 (s, 3H), 1.30 (t, *J* = 7.0 Hz, 1H). ESI-MS: *m/z*=322 $[M+H]^+$.

General Synthetic Procedure for compound 7a-7j

A mixture of **13a-13g** (0.5 mmol), secondary amine (pyrrolidine, or piperidine, or morpholine, or N-methylpiperazine, 1.5 mmol) and triethylamine (0.4 mL, 2.5 mmol) was refluxed overnight in 10 mL acetonitrile. The mixture was concentrated to dryness and the residue was partitioned between ethyl acetate (20 mL) and 2.0 mol/L hydrochloric acid (20 mL). The organic layers were discarded and the aqueous layer was basified with 2.0 mol/L NaOH (pH > 10) and extraction with EtOAc (20 mL×3). The combined organic layer was washed with brine, dried over Na_2SO_4, and concentrated to dryness in vacuo. The residue was purified by silica gel chromatography to give **7a-7j**.

3-Methoxy-2-methyl-1-(4-(3-(pyrrolidin-1-yl)propoxy)phenyl)pyridin-4(1H)-one (7a)

Pale-yellow solid, yield 61%, mp 89℃. IR (KBr, cm^{-1}) 3029, 2995, 2949, 2878, 1621, 1557, 1508, 1288, 1239, 1052, 840. ^{1}H NMR (500 MHz, $CDCl_3$): δ 7.19 (d, *J* = 7.5Hz, 1H), 7.09 (d, *J* = 9.0 Hz, 2H), 6.93 (d, *J* = 9.0 Hz, 2H), 6.38 (d, *J* = 7.5 Hz, 1H), 4.05 (t, *J* = 6.5 Hz, 2H), 3.84 (s, 3H), 2.70 (t, *J* = 7.0 Hz, 2H), 2.62-2.59 (m, 4H), 2.07-2.01 (m, 2H), 1.99 (s, 3H), 1.82-1.78 (m, 4H). ^{13}C NMR (125 MHz, $CDCl_3$): δ 173.74, 159.54, 147.36, 141.11, 139.01, 134.46, 127.82, 116.84, 115.42, 66.49, 59.41, 54.24, 52.96, 28.67, 23.44, 14.07. HRMS (ESI) *m/z* Calcd. for $C_{20}H_{27}N_2O_3^+$ $[M+H]^+$ 343.2016, Found 343.2024. HPLC purity: 98.5%.

3-Methoxy-2-methyl-1-(4-(3-(piperidin-1-yl)propoxy)phenyl)pyridin-4(1H)-one (7b)

Pale-yellow solid, yield 82%, mp 89℃. IR (KBr, cm^{-1}) 3071, 2967, 2929, 2883, 1623, 1573, 1508, 1286, 1248, 1045, 836. ^{1}H NMR (500 MHz, $CDCl_3$): δ 7.20 (d, *J* = 7.5Hz, 1H), 7.10 (d, *J* = 9.0 Hz, 2H), 6.93 (d, *J* = 9.0 Hz, 2H), 6.38 (d, *J* = 7.5 Hz, 1H), 4.03 (t, *J* = 6.5 Hz, 2H), 3.84 (s, 3H), 2.58 (t, *J* = 7.0 Hz, 2H), 2.53-2.47 (m, 4H), 2.07-2.01 (m, 2H), 1.99 (s, 3H), 1.64-1.61 (m, 4H),

1.44-1.42 (m, 2H). ^{13}C NMR (125 MHz, $CDCl_3$): δ 173.74, 159.54, 147.34, 141.20, 139.04, 134.43, 127.81, 116.80, 115.42, 66.92, 59.41, 55.77, 54.60, 26.57, 25.81, 24.29, 14.07. HRMS (ESI) *m/z* Calcd. for $C_{21}H_{29}N_2O_3^+$ $[M+H]^+$ 357.2173, Found 357.2182. HPLC purity: 97.5%.

3-Methoxy-2-methyl-1-(4-(3-morpholinopropoxy)phenyl)pyridin-4(1H)-one (7c)

Pale-yellow solid, yield 81%, mp 87℃. IR (KBr, cm^{-1}) 3065, 2974, 2936, 2897, 1620, 1556, 1508, 1288, 1238, 1052, 843. ^{1}H NMR (500 MHz, $CDCl_3$): δ 7.21 (d, *J* = 7.5Hz, 1H), 7.10 (d, *J* = 9.0 Hz, 2H), 6.93 (d, *J* = 9.0 Hz, 2H), 6.41 (d, *J* = 7.5 Hz, 1H), 4.03 (t, *J* = 6.5 Hz, 2H), 3.84 (s, 3H), 3.69-3.65 (m, 4H), 2.51 (t, *J* = 7.0 Hz, 2H), 2.47-2.41 (m, 4H), 2.00 (s, 3H), 1.98-1.93 (m, 2H). ^{13}C NMR (125 MHz, $CDCl_3$): δ 173.73, 159.51, 147.35, 141.38, 139.14, 134.50, 127.84, 116.80, 115.43, 66.74, 66.52, 59.49, 55.37, 53.64, 26.12 , 14.09. HRMS (ESI) *m/z* Calcd. for $C_{20}H_{27}N_2O_4^+$ $[M+H]^+$ 359.1965, Found 359.1971. HPLC purity: 98.4%.

3-Methoxy-2-methyl-1-(4-(3-(4-methyl-1-piperazinyl)propoxy)phenyl)pyridin-4(1H)-one (7d)

Pale-yellow solid, yield: 64%, mp 95℃. ^{1}H NMR (400 MHz, $CDCl_3$): δ 7.27 (d, *J* = 7.6Hz, 1H), 7.17 (d, *J* = 8.8Hz, 2H), 7.00 (d, *J* = 8.8 Hz, 2H), 6.46 (d, *J* = 7.6 Hz, 1H), 4.09 (t, *J* = 6.0 Hz, 2H), 3.91 (s, 3H), 2.60-2.56 (m, 6H), 2.48-2.40 (m, 4H), 2.34 (s, 3H), 2.06 (s, 3H), 2.05-2.00 (m, 2H). ^{13}C NMR (100 MHz, $CDCl_3$): δ 173.77, 159.51, 147.40, 141.15, 139.01, 134.55, 127.86, 116.86, 115.43, 66.66, 59.44, 54.89, 52.84, 45.77, 26.55, 14.07. HRMS (ESI) *m/z* Calcd. for $C_{21}H_{30}N_3O_3^+$ $[M+H]^+$ 372.2282, Found 372.2294. HPLC purity: 97.4%.

3-Methoxy-2-methyl-1-(4-(2-(pyrrolidin-1-yl)ethoxy)phenyl)pyridin-4(1H)-one (7e)

Pale-yellow solid, yield: 70%, mp 90℃. ^{1}H NMR (500 MHz, $CDCl_3$): δ 7.24 (d, *J* = 7.5Hz, 1H), 7.15 (d, *J* = 9.0 Hz, 2H), 7.00 (d, *J* = 9.0 Hz, 2H), 6.43 (d, *J* = 7.5 Hz, 1H), 4.17 (t, *J* = 6.5 Hz, 2H), 3.89 (s, 3H), 2.97 (t, *J* = 7.0 Hz, 2H), 2.68-2.66 (m, 4H), 2.04 (s, 3H), 1.83-1.80 (m, 4H). ^{13}C NMR (100 MHz, $CDCl_3$): δ 173.78, 159.34, 147.39, 141.18, 139.01, 134.67, 127.87, 116.85, 115.52, 67.42, 59.44, 54.82, 54.68, 23.47, 14.07. HRMS (ESI) *m/z* Calcd. for $C_{19}H_{25}N_2O_3^+$ $[M+H]^+$ 329.1860, Found 329.1867. HPLC purity: 97.1%.

3-Methoxy-2-methyl-1-(4-(4-(pyrrolidin-1-yl)butoxy)phenyl)pyridin-4(1H)-one (7f)

Pale-yellow solid, yield: 76%, mp 82℃. ^{1}H NMR (500 MHz, $CDCl_3$): δ 7.27 (d, *J* = 7.5Hz, 1H), 7.16 (d, *J* = 9.0 Hz, 2H), 6.99 (d, *J* = 9.0 Hz, 2H), 6.45 (d, *J* = 7.5 Hz, 1H), 4.05 (t, *J* = 6.5 Hz, 2H), 3.91 (s, 3H), 2.58-2.54 (m, 6H), 2.06 (s, 3H), 1.90-1.84 (m, 2H), 1.82-1.78 (m, 4H), 1.77-1.72 (m, 2H). ^{13}C NMR (100 MHz, $CDCl_3$): δ173.77, 159.58, 147.38, 141.20, 139.03, 134.45, 127.83, 116.83, 115.40, 68.20, 59.43, 56.00, 54.12, 27.20, 25.31, 23.39, 14.06. HRMS (ESI) *m/z* Calcd. for $C_{21}H_{29}N_2O_3^+$ $[M+H]^+$ 357.2173, Found 357.2171. HPLC purity: 96.5%.

2-Ethyl-3-methoxy-1-(4-(3-(pyrrolidin-1-yl)propoxy)phenyl)pyridin-4(1H)-one (7g)

Pale-yellow solid, yield 58%, mp 93℃. IR (KBr, cm^{-1}) 3034, 2956, 2882, 2817, 1633, 1583, 1506, 1487, 1289, 1248, 1015, 846. ^{1}H NMR (500 MHz, $CDCl_3$): δ 7.15-7.12 (m, 3H), 6.93 (d, *J* = 9.0 Hz, 2H), 6.37 (d, *J* = 7.5 Hz, 1H), 4.08 (t, *J* = 6.5 Hz, 2H), 3.90 (s, 3H), 2.94-2.88 (m, 2H), 2.87-2.84 (m, 4H), 2.43 (q, *J* = 7.5 Hz, 2H), 2.19-2.16 (m, 2H), 1.95-1.90 (m, 4H), 0.93 (t, *J* = 7.5 Hz, 3H). ^{13}C NMR (125 MHz, $CDCl_3$): δ 173.37, 159.00, 146.98, 146.24, 136.37, 134.77, 128.51, 117.17, 115.54, 71.74, 65.66, 53.93, 52.69, 26.37, 23.38, 20.13, 8.75. HRMS (ESI) *m/z* Calcd. for $C_{21}H_{29}N_2O_3^+$ $[M+H]^+$ 357.2173, Found 357.2182. HPLC purity: 98.7%.

5-Methoxy-2-methyl-1-(4-(3-(pyrrolidin-1-yl)propoxy)phenyl)pyridin-4(1H)-one (7h)

Pale-yellow solid, yield 64%, mp 133℃. IR (KBr, cm^{-1}) 3046, 2966, 2951, 2843, 1626, 1583, 1554, 1509, 1286, 1243, 1018, 849. ^{1}H NMR (500 MHz, $CDCl_3$): δ 7.12 (d, *J* = 9.0 Hz, 2H), 6.95 (d, *J* = 9.0 Hz, 2H), 6.88 (s, 1H), 6.31 (s, 1H), 4.06 (t, *J* =6.5 Hz, 2H), 3.68 (s, 3H), 2.78-2.74 (m, 2H), 2.68-2.64 (m, 4H), 2.11-2.06 (m, 2H), 1.93 (s, 3H), 1.86-1.80 (m, 4H). ^{13}C NMR (125 MHz, $CDCl_3$): δ 172.85, 159.32, 148.88, 145.93, 134.97, 127.94, 123.14, 116.15, 115.52, 66.39, 56.23, 54.17, 52.94, 27.78, 23.46, 20.12. HRMS (ESI) *m/z* Calcd. for $C_{20}H_{27}N_2O_3^+$ $[M+H]^+$ 343.2016, Found 343.2013. HPLC purity: 98.5%.

3-Methoxy-1-(4-(3-(pyrrolidin-1-yl)propoxy)phenyl)pyridin-4(1H)-one (7i)

Pale-yellow solid, yield 78%, mp 93℃. IR (KBr, cm^{-1}) 3037, 2974, 2952, 2883, 1627, 1557, 1509, 1286, 1243, 1020, 830. ^{1}H NMR (500 MHz, $CDCl_3$): δ 7.47-7.45 (dd, J_1 = 7.5 Hz, J_2 = 2.5 Hz, 1H), 7.27 (d, *J* = 9.0 Hz, 2H), 7.25 (d, *J* = 2.5 Hz, 1H), 6.87 (d, *J* = 9.0 Hz, 2H), 6.45 (d, *J* = 7.5 Hz, 1H), 4.07 (t, *J* = 5.5 Hz, 2H), 3.79 (s, 3H), 3.38-3.35 (m, 4H), 3.10-3.07 (m, 2H), 2.35-2.31 (m,

2H), 2.16-2.12 (m, 4H). ^{13}C NMR (125 MHz, $CDCl_3$): δ 172.31, 158.72, 150.43, 136.93, 136.80, 124.45, 121.31, 115.93, 115.72, 66.30, 56.33, 54.12, 52.91, 31.23, 29.67, 27.57, 23.43. HRMS (ESI) *m/z* Calcd. for $C_{19}H_{25}N_2O_3^+$ $[M+H]^+$ 329.1860, Found 329.1863. HPLC purity: 99.0%.

3-Ethoxy-2-methyl-1-(4-(3-(pyrrolidin-1-yl)propoxy)phenyl)pyridin-4(1H)-one (7j)

Pale-yellow solid, yield 85%, mp 89℃. IR (KBr, cm^{-1}) 3425, 3138, 3053, 2965, 2929, 2876, 2698, 1621, 1565, 1509, 1479, 1285, 1239, 1050, 845. ^{1}H NMR (500 MHz, $CDCl_3$): δ 7.17 (d, *J* = 7.5 Hz, 1H), 7.09 (d, *J* = 9.0 Hz, 2H), 6.92 (d, *J* = 9.0 Hz, 2H), 6.37 (d, *J* = 7.5 Hz, 1H), 4.18 (q, *J* = 7.0 Hz, 2H), 4.03 (t, *J* = 6.0 Hz, 2H), 2.68 (d, *J* = 7.5 Hz, 2H), 2.60-2.58 (m, 4H), 2.04-2.00 (m, 2H), 1.99 (s, 3H), 1.80-1.76 (m, 4H), 1.30 (t, *J* = 7.0 Hz, 3H). ^{13}C NMR (125 MHz, $CDCl_3$): δ 173.88, 159.42, 146.38, 141.05, 138.84, 134.64, 127.84, 116.71, 115.40, 67.19, 66.78, 54.23, 52.96, 28.57, 23.46, 15.65, 14.30. HRMS (ESI) *m/z* Calcd. for $C_{21}H_{29}N_2O_3^+$ $[M+H]^+$ 357.2173, Found 357.2174. HPLC purity: 97.7%.

N-(tert-Butoxycarbonyl)-4-(4-nitrophenoxy)piperidine (15)

N-(tert-Butoxycarbonyl)-4-hydroxypiperidine (1.0 g, 4.97 mmol) was dissolved in anhydrous DMF (5 mL) and cooled to 0 °C. NaH (60%, 300 mg, 7.5 mmol) was added portionwise in 15 min, and then the mixture was stired for a further 30 min at ambient temperature. The mixture was then cooled to 0 °C, and a solution of 4-fluoronitrobenzene **14** (771 mg, 5.5 mmol) in DMF (10 mL) was added dropwise. The reaction mixture was stirred overnight at ambient temperature. After completion of the reaction, water was added, and the aqueous layer was extracted with EtOAc. The combined organic layers were washed with brine, dried over Na_2SO_4 and evaporated to afford 1.3 g **15** as a pale-yellow solid, yield 81%. ^{1}H NMR (500 MHz, $CDCl_3$): δ 8.22 (d, *J* = 9.0 Hz, 2H), 6.97 (d, *J* = 9.0 Hz, 2H), 4.63-4.59 (m, 2H), 3.73-3.68 (m, 2H), 3.41-3.36 (m, 2H), 1.99-1.94 (m, 2H), 1.82-1.76 (m, 2H), 1.48 (s, 9H). ESI-MS: *m/z* =323.2 $[M+H]^+$.

4-(4-Nitrophenoxy)piperidine (16)

A mixture of **15** (1 g, 3.1 mmol) in CH_2Cl_2 (10 mL) was added trifluoroacetic acid (2.5 mL), and stirred overnight at ambient temperature. The mixture was concentrated to dryness and the residue was partitioned between ethyl acetate (20 mL) and 2.0 mol/L NaOH (20 mL). The combined

organic layers were washed with brine, dried over Na_2SO_4, and concentrated to afford 665 mg **16** as pale-yellow liquid, yield 92%. ^{1}H NMR (500 MHz, $CDCl_3$): δ 8.21 (d, *J* = 9.0 Hz, 2H), 6.96 (d, *J* = 9.0 Hz, 2H), 4.56-4.52 (m, 2H), 3.21-3.16 (m, 2H), 2.86-2.82 (m, 2H), 2.11-2.06 (m, 2H), 1.81-1.74 (m, 2H). ESI-MS: *m/z* =223.1 $[M+H]^+$.

General Synthetic Procedure for compound 17a-17c

A mixture of **16** (1 g, 4.5 mmol) and sodium cyanoborohydride (566 mg, 9 mmol) was dissolved in CH_3OH (10 mL), and acetone (or cyclobutanone, or cyclopentanone, 5 mL) and acetic acid (270 mg) were added and stirred at ambient temperature for 2h. After completion of the reaction, the mixture was concentrated to dryness and the residue was partitioned between ethyl acetate (20 mL) and 2.0 mol/L NaOH (20 mL). The combined organic layers were washed with brine, dried over Na_2SO_4, and concentrated to afford **17a-17c**.

1-Isopropyl-4-(4-nitrophenoxy)piperidine (17a)

Yellow solid, yield 89%. ^{1}H NMR (500 MHz, $CDCl_3$): δ 8.19 (d, *J* = 9.0 Hz, 2H), 6.95 (d, *J* = 9.0 Hz, 2H), 4.41-4.45 (m, 1H), 2.80-2.75 (m, 3H), 2.46-2.41 (m, 2H), 2.02-1.99 (m, 2H), 1.87-1.85 (m, 2H), 1.07 (d, *J* = 6.5Hz, 6H). ESI-MS: *m/z* =265.2 $[M+H]^+$.

1-Cyclobutyl -4-(4-nitrophenoxy)piperidine (17b)

Yellow solid, yield 80%. ^{1}H NMR (500 MHz, $CDCl_3$): δ 8.19 (d, *J* = 9.0 Hz, 2H), 6.95 (d, *J* = 9.0 Hz, 2H), 4.49-4.47 (m, 1H), 2.77-2.75 (m, 1H), 2.64-2.61 (m, 2H), 2.24-2.22 (m, 2H), 2.07-2.00 (m, 4H), 1.90-1.87 (m, 4H), 1.70-1.68 (m, 2H). ESI-MS: *m/z* =277.2 $[M+H]^+$.

1-Cyclopentyl -4-(4-nitrophenoxy)piperidine (17c)

Yellow solid, yield 86%. ^{1}H NMR (500 MHz, $CDCl_3$): δ 8.20 (d, *J* = 9.0 Hz, 2H), 6.96 (d, *J* = 9.0 Hz, 2H), 4.48-4.46 (m, 1H), 2.84-2.82 (m, 2H), 2.60-2.59 (m, 1H), 2.46-2.44 (m, 2H), 2.11-2.08 (m, 2H), 1.91-1.88 (m, 4H), 1.72-1.71 (m, 2H), 1.56-1.54 (m, 2H), 1.48-1.46 (m, 2H). ESI-MS: *m/z* =291.2 $[M+H]^+$.

General Synthetic Procedure for compound 8a-8f

A mixture of compound **17a-17c** (3.8 mmol) in methanol (10mL) was added 10%Pd/C (200mg), stirred overnight at ambient temperature under hydrogen atmosphere. After filtered off the catalyst, the filtrate was concentrated to give **18a-18c**, which were used directly without further purification. Then **18a-18c** (1.3 mmol) and **11a** (or **11d**, 1 mmol) was dissolved in 0.5N hydrochloric acid (3 mL), stirred at 170 °C for 30 min using a microwave reactor. After cooling, the mixture was extracted with EtOAc. The combined organic layers were washed with brine, dried over Na_2SO_4 and evaporated. The residue was purified by silica gel chromatography (EtOAc: CH_3OH: TEA = 20: 1: 0.5) to give **8a-8f**.

1-(4-((1-Isopropylpiperidin-4-yl)oxy)phenyl)-3-methoxy-2-methylpyridin-4(1H)-one (8a)

Yellow solid, yield 56%, mp 142℃. ^{1}H NMR (500 MHz, $CDCl_3$): δ 7.25 (d, *J* = 7.5Hz, 1H), 7.15 (d, *J* = 9.0 Hz, 2H), 6.99 (d, *J* = 9.0 Hz, 2H), 6.44 (d, *J* = 7.5 Hz, 1H), 4.37-4.35 (m, 1H), 3.90 (s, 3H), 2.81-2.76 (m, 3H), 2.47-2.43 (m, 2H), 2.08-2.06 (m, 2H), 2.05 (s, 3H), 1.89-1.82 (m, 2H), 1.08 (s, 3H), 1.07 (s, 3H). ^{13}C NMR (125 MHz, $CDCl_3$): δ 173.77, 158.11, 147.34, 141.26, 139.07, 134.36, 127.91, 116.84, 116.59, 73.34, 59.46, 54.54, 45.58, 30.88, 18.38, 14.14. HRMS (ESI) *m/z* Calcd. for $C_{21}H_{29}N_2O_3^+$ $[M+H]^+$ 357.2173, Found 357.2174.

1-(4-((1-Isopropylpiperidin-4-yl)oxy)phenyl)-3-methoxypyridin-4(1H)-one (8b)

Yellow solid, yield 48%, mp 97℃. ^{1}H NMR (500 MHz, $CDCl_3$): δ 7.38 (d, *J* = 7.5Hz, 1H), 7.25 (d, *J* = 9.0 Hz, 2H), 7.20 (s, 1H), 6.95 (d, *J* = 9.0 Hz, 2H), 6.42 (d, *J* = 7.5 Hz, 1H), 4.31-4.29 (m, 1H), 3.80 (s, 3H), 2.71-2.66 (m, 3H), 2.37-2.33 (m, 2H), 2.03-2.01 (m, 2H), 1.84-1.82 (m, 2H), 1.05 (s, 3H), 1.04 (s, 3H). ^{13}C NMR (125 MHz, $CDCl_3$): δ 172.33, 157.50, 150.43, 136.79, 136.74, 124.50, 121.19, 117.04, 115.92, 73.42, 56.26, 54.56, 45.55, 30.85, 18.38. HRMS (ESI) *m/z* Calcd. for $C_{21}H_{29}N_2O_3^+$ $[M+H]^+$ 343.2016, Found 343.2020.

1-(4-((1-Cyclobutylpiperidin-4-yl)oxy)phenyl)-3-methoxy-2-methylpyridin-4(1H)-one (8c)

Yellow solid, yield 53%, mp 153℃. ^{1}H NMR (500 MHz, $CDCl_3$): δ 7.25 (d, *J* = 7.5Hz, 1H), 7.15 (d, *J* = 9.0 Hz, 2H), 6.99 (d, *J* = 9.0 Hz, 2H), 6.44 (d, *J* = 7.5 Hz, 1H), 4.38-4.36 (m, 1H), 3.92 (s, 3H), 2.77-2.76 (m, 1H), 2.66-2.64 (m, 2H), 2.21-2.20 (m, 2H), 2.06-2.00 (m, 7H), 1.88-1.86 (m, 4H), 1.75-1.66 (m, 2H). ^{13}C NMR (125 MHz, $CDCl_3$): δ 173.75, 158.03, 147.36, 141.08, 139.00,

134.42, 127.95, 116.90, 116.57, 72.66, 60.28, 59.45, 46.68, 30.26, 27.45, 14.15. HRMS (ESI) *m/z* Calcd. for $C_{22}H_{29}N_2O_3^+$ $[M+H]^+$ 369.2173, Found 369.2176.

1-(4-((1-Cyclobutylpiperidin-4-yl)oxy)phenyl)-3-methoxypyridin-4(1H)-one (8d)

Yellow solid, yield 51%, mp 152℃. ^{1}H NMR (500 MHz, $CDCl_3$): δ 7.38 (d, *J* = 7.5Hz, 1H), 7.25 (d, *J* = 9.0 Hz, 2H), 7.20 (s, 1H), 6.95 (d, *J* = 9.0 Hz, 2H), 6.42 (d, *J* = 7.5 Hz, 1H), 4.31-4.29 (m, 1H), 3.74 (s, 3H), 2.73-2.66 (m, 1H), 2.57-2.55 (m, 2H), 2.14-2.12 (m, 2H), 1.96-1.92 (m, 4H), 1.84-1.78(m, 4H), 1.65-1.63 (m, 2H). ^{13}C NMR (125 MHz, $CDCl_3$): δ 172.35, 157.40, 150.47, 136.85, 136.76, 124.53, 121.08, 117.05, 115.98, 73.07, 60.28, 56.26, 46.54, 30.07, 27.36, 14.16. HRMS (ESI) *m/z* Calcd. for $C_{21}H_{27}N_2O_3^+$ $[M+H]^+$ 355.2016, Found 355.2025.

1-(4-((1-Cyclopentylpiperidin-4-yl)oxy)phenyl)-3-methoxy-2-methylpyridin-4(1H)-one (8e)

Yellow solid, yield 51%, mp 151℃. ^{1}H NMR (500 MHz, $CDCl_3$): δ 7.25 (d, *J* = 7.5Hz, 1H), 7.15 (d, *J* = 9.0 Hz, 2H), 6.99 (d, *J* = 9.0 Hz, 2H), 6.44 (d, *J* = 7.5 Hz, 1H), 4.38-4.36 (m, 1H), 3.91 (s, 3H), 2.84-2.82 (m, 2H), 2.59-2.54 (m, 1H), 2.42-2.41 (m, 2H), 2.06-2.00 (m, 5H), 1.89-1.87 (m, 4H), 1.72-1.71 (m, 2H), 1.57-1.56 (m, 2H), 1.55-1.52 (m, 2H). ^{13}C NMR (125 MHz, $CDCl_3$): δ 173.76, 158.03, 147.37, 141.12, 139.01, 134.45, 127.96, 116.90, 116.57, 72.90, 67.47, 59.46, 49.38, 30.58, 30.47, 24.21, 14.16. HRMS (ESI) *m/z* Calcd. for $C_{23}H_{31}N_2O_3^+$ $[M+H]^+$ 383.2329, Found 383.2339.

1-(4-((1-Cyclopentylpiperidin-4-yl)oxy)phenyl)-3-methoxypyridin-4(1H)-one (8f)

Yellow solid, yield 44%, mp 157℃. ^{1}H NMR (500 MHz, $CDCl_3$): δ 7.38 (d, *J* = 7.5Hz, 1H), 7.25 (d, *J* = 9.0 Hz, 2H), 7.20 (s, 1H), 6.95 (d, *J* = 9.0 Hz, 2H), 6.42 (d, *J* = 7.5 Hz, 1H), 4.31-4.29 (m, 1H), 3.75 (s, 3H), 2.74-2.72 (m, 2H), 2.55-2.50 (m, 1H), 2.40-2.38 (m, 2H), 2.02-2.00 (m, 2H), 1.85-1.82 (m, 4H), 1.67-1.64 (m, 2H), 1.54-1.53 (m, 2H), 1.52-1.50 (m, 2H). ^{13}C NMR (125 MHz, $CDCl_3$): δ 172.31, 157.46, 150.44, 136.77, 124.50, 121.10, 117.04, 115.92, 73.05, 67.44, 56.24, 49.42, 30.65, 30.55, 24.21. HRMS (ESI) *m/z* Calcd. for $C_{22}H_{29}N_2O_3^+$ $[M+H]^+$ 369.2173, Found 369.2167.

4-(3-Methoxy-2-methyl-4-oxopyridin-1(4H)-yl)benzoic acid (19)

A mixture of methoxymaltol **11a** (1.40 g, 10 mmol), 4-aminobenzoic acid (2.74 g, 20 mmol) was dissolved in C_2H_5OH (10 mL) and H_2O (10 mL), and the reaction was sealed at 150-160 ° C for 12 h. After completion of the reaction, the mixture was cooled, and ethanol was removed under reduced pressure. The precipitate was then filtered and wash with cold ethanol to afford **19** (1.83g) as a whith solid, yield 71%. ^{1}H NMR (400 MHz, DMSO-d6): δ 13.33 (s, 1H), 8.10 (d, J = 8.4 Hz, 2H), 7.64-7.60 (m, 3H), 6.23 (d, J = 7.6 Hz, 2H), 3.76 (s, 3H), 2.00 (s, 3H). ESI-MS: m/z =260 $[M+H]^+$.

N-Boc-3-methoxy-2-methyl-1-(4-(piperazine-1-carbonyl)phenyl)pyridin-4(1H)-one (20)

A mixture of **19** (520 mg, 2 mmol), N-Boc-piperazine (744 mg, 4 mmol) and EDC (460 mg, 2.4 mmol) in dry DMF (5 mL) was added trimethylamine, stirred at ambient temperature for 2h. After completion of the reaction, water (50 mL) was added, and the aqueous layer was extracted with EtOAc (20 mL×3). The combined organic layers were washed with brine, dried over Na_2SO_4 and evaporated to afford **20** as a white solid, which were used directly without further purification.

3-Methoxy-2-methyl-1-(4-(piperazine-1-carbonyl)phenyl)pyridin-4(1H)-one (21)

A mixture of **20** (855 mg, 2 mmol) in CH_2Cl_2 (5 mL) was added trifluoroacetic acid (1 mL), and refluxed for 2h. The mixture was partitioned between CH_2Cl_2 and 10% NaOH. The combined organic layers were washed with brine, dried over Na_2SO_4, and concentrated to afford 370 mg **21** as white solid, yield 57%. ^{1}H NMR (500 MHz, $CDCl_3$): δ 7.60 (d, *J* = 8.5 Hz, 2H), 7.36 (d, *J* = 8.5 Hz, 2H), 7.28 (d, *J* = 7.5 Hz, 1H), 6.51 (d, *J* = 7.5 Hz, 1H), 3.93 (s, 3H), 3.90-3.84 (m, 2H), 3.56-3.50 (m, 2H), 3.08-2.94 (m, 4H), 2.10 (s, 3H). ESI-MS: *m/z* =328 $[M+H]^+$.

General Synthetic Procedure for compound 9a-9c

A mixture of **21** (0.31 mmol) and sodium cyanoborohydride (29 mg, 0.46 mmol) in CH_3OH_2 (3 mL) was added acetone (or cyclobutanone, or cyclopentanone, 0.11mL) and acetic acid (17 μL), and stirred at ambient temperature for 2h. After completion of the reaction, water was added, and the aqueous layer was extracted with EtOAc. The combined organic layers were washed with brine, dried over Na_2SO_4, and concentrated to dryness in vacuo. The residue was purified by silica gel chromatography (EtOAc: CH_3OH: TEA = 10: 1: 0.5) to give **9a-9c**.

1-(4-(4-Isopropylpiperazine-1-carbonyl)phenyl)-3-methoxy-2-methylpyridin-4(1H)-one(9a)

White solid, yield 68%, mp 150℃. ^{1}H NMR (500 MHz, $CDCl_3$): δ 7.59 (d, *J* = 8.5 Hz, 2H), 7.35 (d, *J* = 8.5 Hz, 2H), 7.26 (d, *J* = 7.5 Hz, 1H), 6.47 (d, *J* = 7.5 Hz, 1H), 3.93 (s, 3H), 3.87 (s, 2H), 3.52 (m, 2H), 2.83 (t, *J* = 5.5 Hz, 1H), 2.68-2.56 (m, 4H), 2.09 (s, 3H), 1.11-1.10 (m, 6H). ^{13}C NMR (125 MHz, $CDCl_3$): δ173.73, 167.74, 147.46, 141.79, 140.68, 138.60, 138.10, 131.37, 129.99, 129.59, 116.99, 65.58, 59.49, 52.66, 30.57, 19.19, 14.16. HRMS (ESI) *m/z* Calcd. for $C_{21}H_{28}N_3O_3^+$ $[M+H]^+$ 370.2125, Found 370.2130.

1-(4-(4-Isopropylpiperazine-1-carbonyl)phenyl)-3-methoxy-2-methylpyridin-4(1H)-one (9b)

White solid, yield 58%, mp 216℃. ^{1}H NMR (500 MHz, $CDCl_3$): δ 7.58 (d, *J* = 8.5 Hz, 2H), 7.35 (d, *J* = 8.5 Hz, 2H), 7.25 (d, *J* = 7.5 Hz, 1H), 6.47 (d, *J* = 7.5 Hz, 1H), 3.93 (s, 3H), 3.87 (s, 2H), 3.51 (s, 2H), 2.86-2.80 (m, 1H), 2.49-2.38 (m, 4H), 2.09-2.05 (m, 5H), 1.97-1.94 (m, 2H), 1.80-1.69(m, 2H). ^{13}C NMR (125 MHz, $CDCl_3$): δ173.82, 168.53, 147.59, 142.69, 140.23, 138.29, 136.99, 130.93, 128.88, 127.19, 117.27, 65.59, 60.01, 59.50, 26.72, 19.19, 14.26, 14.22. HRMS (ESI) *m/z* Calcd. for $C_{22}H_{28}N_3O_3^+$ $[M+H]^+$ 382.2125, Found 382.2138.

1-(4-(4-Isopropylpiperazine-1-carbonyl)phenyl)-3-methoxy-2-methylpyridin-4(1H)-one (9c)

White solid, yield 61%, mp 234℃. ^{1}H NMR (400 MHz, $CDCl_3$): δ 7.60 (d, *J* = 8.4 Hz, 2H), 7.36 (d, *J* = 8.4 Hz, 2H), 7.31 (d, *J* = 7.6 Hz, 1H), 6.50 (d, *J* = 7.6 Hz, 1H), 3.92 (s, 3H), 3.86-3.80 (m, 2H), 3.54-3.46 (m, 2H), 2.66-2.48 (m, 5H), 2.10 (s, 3H), 1.90-1.85 (m, 2H), 1.74-1.69 (m, 2H), 1.60-1.56 (m, 2H), 1.46-1.40 (m, 2H). ^{13}C NMR (125 MHz, $CDCl_3$): δ173.75, 168.32, 147.52, 142.53, 140.12, 138.21, 137.14, 128.80, 127.07, 117.21, 67.19, 59.42, 52.50, 51.76, 30.28, 24.00, 14.18. HRMS (ESI) *m/z* Calcd. for $C_{23}H_{30}N_3O_3^+$ $[M+H]^+$ 396.2282, Found 396.2289.

N-Boc-4-((4-nitrophenyl)sulfonyl)piperazine-1-carboxylate (23)

A mixture of N-Boc-piperazine (3.05 g, 16.4 mmol) and DIPEA (3.14 mL, 18 mmol) in dry CH_2Cl_2 (20 mL) was added **22** (3.99 g, 18 mmol) in portions, stired under nitrogen atmosphere at ambient temperature for 1h. After completion of the reaction, water was added, and the aqueous layer was extracted with CH_2Cl_2. The combined organic layers were washed with brine, dried over

Na_2SO_4, and concentrated to afford 6.0g **23** as a white solid, yield 99%. ^{1}H NMR (500 MHz, $CDCl_3$): δ 8.41 (d, *J* = 9.0 Hz, 2H), 7.96 (d, *J* = 9.0 Hz, 2H), 3.55 (t, *J* = 5.0 Hz, 4H), 3.05 (t, *J* = 5.0 Hz, 4H), 1.41 (s, 9H). ESI-MS: *m/z* =372 $[M+H]^+$.

4-((4-nitrophenyl)sulfonyl)piperazine-1-carboxylate (24)

A mixture of **23** (5.45 g, 14.6 mmol) in CH_2Cl_2 (25 mL) was added trimethylamine at 0℃, and then stirred at ambient temperature overnight. After completion of the reaction, the mixture was concentrated to dryness and the residue was partitioned between ethyl acetate (20 mL) and 2.0 mol/L NaOH (20 mL). The combined organic layers were washed with brine, dried over Na_2SO_4, and concentrated to afford 3.6g **24** as a yellow solid, yield 91%. ^{1}H NMR (500 MHz, $CDCl_3$): δ 8.41 (d, *J* = 9.0 Hz, 2H), 7.96 (d, *J* = 9.0 Hz, 2H), 3.06 (t, *J* = 5.0 Hz, 4H), 2.96 (t, *J* = 5.0 Hz, 4H). ESI-MS: *m/z* =272 $[M+H]^+$.

General Synthetic Procedure for compound 26a-26c

A mixture of **24** (4.5 mmol) and sodium cyanoborohydride (9 mmol) was dissolved in CH_3OH (10 mL), and acetone (or cyclobutanone, or cyclopentanone, 5 mL) and acetic acid (270 mg) were added and stirred at ambient temperature for 2h. After completion of the reaction, the mixture was concentrated to dryness and the residue was partitioned between ethyl acetate (20 mL) and 2.0 mol/L NaOH (20 mL). The combined organic layers were washed with brine, dried over Na_2SO_4, and concentrated to afford **25a-25c**. A mixture of compound **25a-25c** (3.8 mmol) in methanol (10mL) was added 10%Pd/C (200mg), stirred overnight at ambient temperature under hydrogen atmosphere. After filtered off the catalyst, the filtrate was concentrated and purified by silica gel chromatography (EtOAc: CH_3OH: TEA = 20: 1: 0.5) to give **26a-26c**.

4-((4-Isopropylpiperazin-1-yl)sulfonyl)aniline (26a)

Yellow solid, yield 93%. ^{1}H NMR (500 MHz, DMSO-d_6): δ 7.34 (d, *J* = 8.5 Hz, 2H), 6.66 (d, *J* = 8.5 Hz, 2H), 6,12 (s, 2H), 2.82-2.76 (m, 4H), 2.64-2.58 (m, 1H), 2.50-2.45 (m, 4H), 1.01 (s, 6H). ESI-MS: *m/z* =284 $[M+H]^+$.

4-((4-Cyclobutylpiperazin-1-yl)sulfonyl)aniline (26b)

White solid, yield 61%. ^{1}H NMR (500 MHz, DMSO-d_6): δ 7.34 (d, *J* = 8.5 Hz, 2H), 6.66 (d, *J* = 8.5 Hz, 2H), 6,12 (s, 2H), 2.81-2.75 (m, 4H), 2.69-2.62 (m, 1H), 2.28-2.24 (m, 4H), 1.92-1.88 (m, 2H), 1.70-1.62 (m, 2H), 1.60-1.54 (m, 2H). ESI-MS: *m/z* =295 $[M+H]^+$.

4-((4-Cyclopentylpiperazin-1-yl)sulfonyl)aniline (26c)

White solid, yield 78%. ^{1}H NMR (500 MHz, DMSO-d_6): δ 7.34 (d, *J* = 8.5 Hz, 2H), 6.65 (d, *J* = 8.5 Hz, 2H), 6,12 (s, 2H), 2.81-2.75 (m, 4H), 2.46-2.42 (m, 5H), 1.74-1.68 (m, 2H), 1.58-1.51 (m, 2H), 1.48-1.42 (m, 2H), 1.24-1.18 (m, 2H). ESI-MS: *m/z* =310 $[M+H]^+$.

General Synthetic Procedure for compound 10a-10c

26a-26c (1.3 mmol) and **11a** (1 mmol) was dissolved in 0.5N hydrochloric acid (2 mL) and C_2H_5OH(0.5 mL), stirred at 160 °C for 30 min using a microwave reactor. After cooling, the mixture was extracted with EtOAc. The combined organic layers were washed with brine, dried over Na_2SO_4 and evaporated. The residue was purified by silica gel chromatography (EtOAc: CH_3OH: TEA = 20: 1: 0.5) to give **10a-10c**.

1-(4-((4-Isopropylpiperazin-1-yl)sulfonyl)phenyl)-3-methoxy-2-methylpyridin-4(1H)-one (10a)

White solid, yield 45%, mp 90℃. ^{1}H NMR (500 MHz, $CDCl_3$): δ 7.87 (d, *J* = 8.5 Hz, 2H), 7.43 (d, *J* = 8.5 Hz, 2H), 7.19 (d, *J* = 7.5 Hz, 1H), 6.42 (d, *J* = 7.5 Hz, 1H), 3.86 (s, 3H), 3.18-3.09 (m, 4H), 2.70-2.60 (m, 5H), 2.02 (s, 3H), 1.02 (s, 6H). ^{13}C NMR (125 MHz, $CDCl_3$): δ173.49, 147.42, 144.98, 139.29, 137.60, 136.64, 129.34, 127.55, 117.28, 59.18, 47.37, 45.73, 29.38, 17.81, 14.02. HRMS (ESI) *m/z* Calcd. for $C_{20}H_{28}N_3O_4S^+$ $[M+H]^+$ 406.1795, Found 406.1796.

1-(4-((4-Cyclobutylpiperazin-1-yl)sulfonyl)phenyl)-3-methoxy-2-methylpyridin-4(1H)-one (10b)

White solid, yield 52%, mp 124℃. ^{1}H NMR (500 MHz, $CDCl_3$): δ 7.86 (d, *J* = 8.5 Hz, 2H), 7.42 (d, *J* = 8.5 Hz, 2H), 7.16 (d, *J* = 7.5 Hz, 1H), 6.43 (d, *J* = 7.5 Hz, 1H), 3.87 (s, 3H), 3.12-3.05 (m, 4H), 2.72-2.69 (m, 1H), 2.42-2.36 (m, 4H), 2.02 (s, 3H), 2.00-1.96 (m, 2H), 1.76-1.68 (m, 2H), 1.68-1.62 (m, 2H). ^{13}C NMR (125 MHz, $CDCl_3$): δ173.78, 147.75, 145.24, 139.49, 137.84, 137.01,

129.67, 127.77, 117.63, 59.64, 59.48, 48.44, 45.88, 26.97, 14.31, 14.10. HRMS (ESI) *m/z* Calcd. for $C_{21}H_{28}N_3O_4S^+$ $[M+H]^+$ 418.1795, Found 418.1800.

1-(4-((4-Cyclopentylpiperazin-1-yl)sulfonyl)phenyl)-3-methoxy-2-methylpyridin-4(1H)-one (10c)

White solid, yield 43%, mp 118℃. ^{1}H NMR (500 MHz, $CDCl_3$): δ 7.86 (d, *J* = 8.5 Hz, 2H), 7.41 (d, *J* = 8.5 Hz, 2H), 7.17 (d, *J* = 7.5 Hz, 1H), 6.43 (d, *J* = 7.5 Hz, 1H), 3.87 (s, 3H), 3.12-3.05 (m, 4H), 2.62-2.46 (m, 5H), 2.02 (s, 3H), 1.85-1.78 (m, 2H), 1.65-1.58 (m, 2H), 1.50-1.47 (m, 2H), 1.30-1.25 (m, 2H). ^{13}C NMR (125 MHz, $CDCl_3$): δ173.79, 147.75, 145.27, 139.53, 137.85, 136.87, 129.71, 127.78, 117.63, 69.97, 59.49, 51.16, 45.99, 30.27, 24.02, 14.33. HRMS (ESI) *m/z* Calcd. for $C_{22}H_{30}N_3O_4S^+$ $[M+H]^+$ 432.1952, Found 432.1966.

References

[1] M. Wortmann, World Alzheimer Report 2018: The state of the art of dementia research: New frontiers, Alzheimer's Dement 2018.

[2] R. Anand, K.D. Gill, A.A. Mahdi, Therapeutics of Alzheimer's disease: Past, present and future, Neuropharmacology 76 (2014) 27-50.

[3] C. Ballard, S. Gauthier, A. Corbett, C. Brayne, D. Aarsland, E. Jones, Alzheimer's disease, Lancet 377 (2011) 1019-1031.

[4] P. Raina, P. Santaguida, A. Ismaila, C. Patterson, D. Cowan, M. Levine, L. Booker, M. Oremus, Effectiveness of cholinesterase inhibitors and memantine for treating dementia: Evidence review for a clinical practice guideline, Ann. Intern. Med. 148 (2008) 379-397.

[5] A. Takeda, E. Loveman, A. Clegg, J. Kirby, J. Picot, E. Payne, C. Green, A systematic review of the clinical effectiveness of donepezil, rivastigmine and galantamine on cognition, quality of life and adverse events in Alzheimer's disease, Int. J. Geriatr. Psychiatry 21 (2006**)** 17-28.

[6] H.W. Querfurth, F.M. LaFerla, Alzheimer's disease, N. Engl. J. Med. 362 (2010) 329-344.

[7] K.A. Jellinger, Alzheimer 100-highlights in the history of Alzheimer research, Journal of Neural Transmission 113 (2006) 1603-1623.

[8] E.D. Roberson, L. Mucke, 100 years and counting: prospects for defeating Alzheimer's disease, Science 314 (2006) 781-784.

[9] M. Citron, Alzheimer's disease: strategies for disease modification, Nat. Rev. Drug Discov. 9 (2010) 387-398.

[10] R. Leon, A.G. Garcia, J. Marco Contelles, Recent advances in the multitargetdirected ligands approach for the treatment of Alzheimer's disease, Med. Res. Rev. 33 (2013) 139-189.

[11] M. Bajda, N. Guzior, M. Ignasik, B. Malawska, Multi-target-directed ligands in Alzheimer's disease treatment, Curr. Med. Chem. 18 (2011) 4949-4975.

[12] L. Ismaili, M.D. Carreiras, Multi-component Reactions for Multitargeted Compounds for Alzheimer's Disease, Curr. Top. Med. Chem. 17 (2018) 3319-3327.

[13] Y.Y. Syed, Sodium Oligomannate: First Approval, Drugs 80 (2020) 441-444.

[14] S. Chakraborty, Multi-potent Natural Scaffolds Targeting Amyloid Cascade: In Search of Alzheimer's Disease Therapeutics, Curr. Top. Med. Chem. 17 (2018) 3336-3348.

[15] E. Tiligada, K. Kyriakidis, P.L. Chazot, M.B. Passani, Histamine pharmacology and new CNS drug targets, CNS Neurosci. Ther. 17 (2011) 620-628.

[16] M. Berlin, C.W. Boyce, M. de Lera Ruiz, Histamine H3 receptor as a drug discovery target, J. Med. Chem. 54 (2011) 26-53.

[17] M. Bhowmik, R. Khanam, D. Vohora, Histamine H_3 receptor antagonists in relation to epilepsy and neurodegeneration: a systemic consideration of recent progress and perspectives, Br. J. Pharmacol. 167 (2012) 1398-1414.

[18] D. Łazewska, K. Kiec-Kononowicz, New developments around histamine H_3 receptor antagonists/inverse agonists: a patent review (2010-present), Expert Opin. Ther. Pat. 24 (2014) 89-111.

[19] Y.Y. Syed, Pitolisant: First Global Approval, Drugs 76 (2016) 1313-1318.

[20] Y.N. Lamb, Pitolisant: A Review in Narcolepsy with or without Cataplexy, CNS Drugs. 34 (2020) 207-218.

[21] J. Hardy, D.J. Selkoe, The amyloid hypothesis of alzheimer's disease: progress and problems on the road to therapeutics, Science 297 (2002) 353-356.

[22] H.F. Kung, The β-amyloid hypothesis in Alzheimer's disease: seeing is believing, ACS Med. Chem. Lett. 3 (2012) 265-267.

[23] A.S. DeToma, S. Salamekh, A. Ramamoorthy, M.H. Lim, Misfolded proteins in Alzheimer's disease and type II diabetes, Chem. Soc. Rev. 41 (2012) 608-621.

[24] R. Jakob-Roetne, H. Jacobsen, Alzheimer's disease: from pathology to therapeutic approaches, Angew. Chem. Int. Ed. 48 (2009) 3030-3059.

[25] I.W. Hamley, The amyloid beta peptide: a chemist's perspective. Role in alzheimer's and fibrillization, Chem. Rev. 112 (2012) 5147-5192.

[26] B.J. Gilbert, The role of amyloid beta in the pathogenesis of Alzheimer's disease, Postgrad. Med. J. 90 (2014) 113–117.

[27] F. Chiti, C.M. Dobson, Protein misfolding, functional amyloid, and human disease, Ann. Rev. Biochem. 75 (2006) 333-366.

[28] R. Sheng, L. Tang, L. Jiang, L. Hong, Y. Shi, N. Zhou, Y. Hu, Novel 1-Phenyl-3-hydroxy-4-pyridinone derivatives as multifunctional agents for the therapy of Alzheimer's Disease, ACS Chem. Neurosci. 7 (2016) 69-81.

[29] L. Di, The role of drug metabolizing enzymes in clearance, Expert Opin. Drug Metabol. Toxicol. 10 (2014) 379-393.

[30] M.O. Benoit-Biancamano, J. Connelly, L. Villeneuve, P. Caron, C. Guillemette, Deferiprone Glucuronidation by Human Tissues and Recombinant UDP Glucuronosyltransferase 1A6: An in Vitro Investigation of Genetic and Splice Variants, Drug Metab. Dispos. 37 (2009) 322-329.

[31] R.H. Lee, C.J. Heckman, Enhancement of bistability in spinal motoneurons in vivo by the noradrenergic alpha1 agonist methoxamine, J. Neurophysiol. 81 (1999) 2164-2174.

[32] T. Shimamura, M. Shiroishi, S. Weyand, H. Tsujimoto, G. Winter, V. Katritch, R. Abagyan, C V. herezov, W. Liu, G.W. Han, T. Kobayashi, R.C. Stevens, S. Iwata, Structure of the human histamine H1 receptor complex with doxepin, Nature 475 (2011) 65−70.

[33] O. Crescenzi, S. Tomaselli, R. Guerrini, S. Salvadori, A.M. D'Ursi, P.A. Temussi, D. Picone, Solution structure of the Alzheimer amyloid beta-peptide (1−42) in an apolar microenviron-ment. Similarity with a virus fusion domain, Eur. J. Biochem. 269 (2002) 5642−5648.

[34] G.B. Fox, J.B. Pan, T.A. Esbenshade, R.S. Bitner, A.L. Nikkel, T. Miller, C.H. Kang, Y.L. Bennani, L.A. Black, R. Faghih, A.A. Hancock, M.W. Decker, Differential in vivo effects of H3 receptor ligands in a new mouse dipsogenia model, Pharmacol. Biochem. Behav. 72 (2002) 741-750.

[35] V.A. Komater, M.J. Buckley, K.E. Browman, J.B. Pan, A.A. Hancock, M.W. Decker, G.B. Fox, Effects of histamine H-3 receptor antagonists in two models of spatial learning, Behavioural Brain Research 159 (2005) 295–300.

Declaration of interests

☒ The authors declare that they have no known competing financial interests or personal relationships that could have appeared to influence the work reported in this paper.

☐The authors declare the following financial interests/personal relationships which may be considered as potential competing interests:

Highlights

- Twenty two *N*-phenyl-3-methoxy-4-pyridione derivatives were designed, synthesized and evaluated as dual functional agents for Alzheimer's Disease with improved orally bioavailability through blocking the phase II metabolism of the 3-hydroxy-4-pyridinone moiety in lead compound **4**.
- Compound **7i** exhibited potent H_3R antagonistic activity and good selectivity over other three histamine receptors, accompanied with good Aβ aggregation inhibition and low hERG inhibtion.
- Compound **7i** displayed a good oral bioavailability of 47.9% and demonstrated good efficacy in (R)-α-methylhistamine-induced dipsogenia model as well as scopolamine-induced learning deficits model *in vivo*.